J|A|C|S ARTICLES

Published on Web 06/19/2009

Desulfinylation of Prop-2-enesulfinic Acid: Experimental Results and Mechanistic Theoretical Analysis

Adrián Varela-Álvarez,[†] Dean Marković,[‡] Pierre Vogel,*[,‡] and José Ángel Sordo*[,†]

Laboratorio de Química Computacional, Departamento de Química Física y Analítica, Universidad de Oviedo, Principado de Asturias, Spain, and Laboratoire de glycochimie et de synthèse asymétrique (LGSA), Swiss Federal Institute of Technology of Lausanne (EPFL), CH 1015 Lausanne, Switzerland

Received February 28, 2009; E-mail: jasg@uniovi.es (J.Á.S.); pierre.vogel@epfl.ch (P.V.)

Abstract: The potential energy surfaces of the desulfinylation of prop-2-enesulfinic acid (**13**) in CH_2Cl_2 solution at −15 °C have been explored by quantum calculations and analyzed with kinetic data obtained for the reaction in absence or presence of additives. Monomeric **13** adopts a preferred conformation with gauche S=O/σ(C(1)−C(2) bond pairs and the O−H bond pointing toward C(3). It equilibrates with the more stable dimer (**13**)$_2$ (at −15 °C) formed by two O−H···O=S hydrogen bonds and in which the S=O/σC(1)−C(2) are gauche also, but the SOH moieties are antiperiplanar with respect to σ(C(1)−C(2)). Dimer (**13**)$_2$ undergoes desulfinylation into propene + SO_2 + **13** following a one-step, concerted mechanism. The preferred transition state is a six-membered, chairlike transition structure (C···S elongation and S−O···H···C(3) hydrogen transfer occur in concert) in which the S=O/σ(C(1)−C(2)) bonds are gauche (S=O adopt pseudoaxial positions). There are at least 48 transition states, each one defining a different pathway, all with similar calculated free energies ($\Delta G^{\ddagger}$ = 25.3−28.6 kcal/mol), which makes the bimolecular (autocatalyzed) retro-ene elimination of SO_2 competing (entropy factor) with a monomolecular process for which the transition state (calculated $\Delta G^{\ddagger}$ = 24.3 kcal/mol) implies only one molecule of sulfinic acid. This agrees with the experimental rate law of the reaction which is first order in the concentration of dimer (**13**)$_2$. SO_2, CF_3COOH, and $BF_3\cdot Me_2O$ do not catalyze the reaction. In the presence of an excess of $BF_3\cdot Me_2O$ the desulfinylation is completely inhibited due to the formation of a stable tetramolecular complex of type (CH_2=$CHCH_2SO_2H\cdot BF_3$)$_2$ (**18**), for which quantum calculations show that the S=O/σ(C(1)−C(2)) bonds are antiperiplanar whereas the S−OH/σ(C(1)−C(2)) bonds are gauche. Independently of the additive, the retro-ene eliminations of SO_2 are calculated to be concerted and have transition states adopting six-membered cyclic structures in which S=O and σ(C(1)−C(2)) are gauche, the S=O interacting with the additive. Preliminary experiments suggested that the thermodynamically unfavored ene reaction of SO_2 with propene can occur at low temperature using 1 equiv of BF_3.

Introduction

The thermal desulfinylation of β,γ-unsaturated sulfinic acids is a useful reaction for the regio- and stereoselective synthesis of alkenes (Scheme 1).[1] In the case of α-substituted sulfinic acids **1**, a concerted retro-ene reaction (formally a retro hetero-Alder[2,3] ene reaction) that leads to the elimination of SO_2 is assumed to be responsible for the chirality transfer from the α-carbon center to the γ-carbon center with formation of alkenes **3**. The stereoselectivity of the reaction is explained in terms of a chairlike transition state **2**[4] that places an optimal number of substituents in pseudoequatorial positions.[5−11] Kinetic investigations by Young and co-workers[4,12] on the desulfinylation of prop-2-enesulfinic acid in toluene were taken as consistent with a cyclic transition state (k_{297K} = 5.5 ± 0.1) × 10^{-4} s^{-1}, $\Delta S^{\ddagger}$ = −35 ± 4.5 e.u.; $\Delta V^{\ddagger}$ = −5.5 ± 1.0 cm^3/mol, ΔV_r = 15 ± 5 cm^3/mol).

Scheme 1

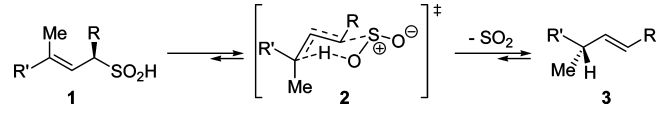

A relatively small deuterium kinetic isotope effect (k_H/k_D = 2.5 ± 0.1) for the H/D transfer also supported the concerted

[†] University of Oviedo.
[‡] Swiss Federal Institute of Technology of Lausanne.

(1) Braverman, S. In *The chemistry of sulfinic acids, esters and their derivatives*; Patai, S., Ed.; Wiley: Chichester, UK, 1990; pp 298−303.
(2) Alder, K.; Pascher, F.; Schmitz, A. *Chem. Ber.* **1943**, *76*, 27–53.
(3) Hoffmann, H. M. R. *Angew. Chem., Int. Ed. Engl.* **1969**, *8*, 556–557.
(4) Hiscock, S. D.; Isaacs, N. S.; King, M. D.; Sue, R. E.; White, R. H.; Young, D. J. *J. Org. Chem.* **1995**, *60*, 7166–7169.
(5) Mock, W. L.; Nugent, R. M. *J. Org. Chem.* **1978**, *43*, 3433–3434.
(6) Garigipati, R. S.; Morton, J. A.; Weinreb, S. M. *Tetrahedron Lett.* **1983**, *24*, 987–990.
(7) Corey, E. J.; Engler, T. A. *Tetrahedron Lett.* **1984**, *25*, 149–152.
(8) Baudin, J. B.; Julia, S. A. *Tetrahedron Lett.* **1988**, *29*, 3255–3258.
(9) Baudin, J. B.; Julia, S. *Bull. Soc. Chim. Fr.* **1995**, *132*, 196–214.
(10) Chochrek, P.; Kurek-Tyrlik, A.; Wicha, J. *Pol. J. Chem.* **2006**, *80*, 679–683.
(11) Chochrek, P.; Wicha, J. *Eur. J. Org. Chem.* **2007**, *253*, 4–2542.

Table 1. Examples of Hetero Ene and Retro-ene Reactions (Estimated Standard Heat of Reactions (25 °C, 1 atm, gas phase), ΔH_r°(in kcal/mol), for Propene (RH=CH_3CH=CH_2) Reacting with Heteroenophiles)

			ΔH_r°	observed reaction T
R-H + SO_2	a) ⇌	R−S(=O)OH	-3.6[f]	<20 °C
R-H + SO	b) c) ⇌	R-SOH	-28.7[f]	not observed
R-H + SO_3	b) ⇌	R-SO_3H	-31.4[f]	<20 °C
R-H + $^1O_2$ ($^1\Delta_g$)	b) ⇌	R-OOH	-35.9[k]	<20 °C
R-H + HN=NH	b) ⇌	R-$NHNH_2$	-15.6[f]	<20 °C[h]
R-H + H-N=O	b) ⇌	R-NHOH	-28[g]	<20 °C[i]
R-H + N≡N	a) ⇌	R-N=NH	+64.6[f]	20 °C[j]
R-H + SeO_2	a) ⇌	R-SeOOH	-13.5	20 °C[g]
R-H + CO_2	a) ⇌	R-COOH	+5.3[f]	>300 °C
R-H + CH_2=O	a) ⇌	R-CH_2-OH	-13.2[f]	>350 °C
R-H + H_2C=NH	a) b) ⇌	R-CH_2-NH_2	-13.6[f]	>325 °C[l]
R-H + H_2C=S	d) ⇌	R-CH_2-SH	-19.	[g]
R-H + HC(OH)=O	c) d) ⇌	R-CHO + H_2O	+8.2[f]	[c]
R-H + C=O	c) e) ⇌	[R$\ddot{C}$OH] → RCHO	+3.5[f]	>300 °C

[a] Follows a concerted mechanism with a six-center transition state for the thermal, non catalyzed reaction (Scheme 2A). [b] Several step process that can imply different type of intermediates (Scheme 2B). [c] Not observed yet. [d] Few examples, mechanism unknown. [e] See decarbonylation of 2,2-dimethyl-3-butenal.[65] [f] Using standard heat of formation (25 °C, 1 atm. gas phase) from ref 14. [g] See text. [h] For electron-poor derivatives.[22] [i] For electron-poor arylNO.[22] [j] See ref 50. [k] For $^1O_2$, using $\Delta H_f^\circ(^1O_2) - \Delta H^\circ(^3O_2) = -22.5$ kcal/mol [l] See TsN=$CHCCl_3$.[22]

mechanism with a relatively compact, early transition state. Alk-2-ene sulfinic acids are generally unstable[1] as they undergo exergonic desulfinylation at room temperature. The difference in standard heats of formation in the gas phase between sulfinic acids (RSO_2H) and the corresponding hydrocarbons (RH) is estimated to be −74.5 kcal/mol.[13] Considering $\Delta H_f^\circ(SO_2, \text{gas}) = -70.9$ kcal/mol,[14] the ene reaction of SO_2 with propene has an exothermicity (standard heat of SO_2 hydrocarbation) of −74.5 + 70.9 = −3.6 kcal/mol in the gas phase (Table 1), what is insufficient to compensate for the cost of entropy of condensation at temperatures higher than −100 °C. Products of ene-reaction have been reported for SO_2 reacting with allenes giving the corresponding 1,3-butadiene-2-sulfinic acids[15] (exothermicity of ca. −14 kcal/mol is estimated in this case) and for SO_2 reacting with 6-alkylidenecyclohexa-1,3-diene derivatives producing corresponding-1-phenylalkane-1-sulfinic acid[16] (gain in aromaticity). At this stage it is interesting to compare the ene-reaction of SO_2 with other related heteroene-reactions (*N*-sulfinylbenzenesulfonamides and *N*-sulfinyl-nonafluorobutanesulfonamide under go easy ene-reactions with alkenes, see refs 17−22).

Scheme 2. Possible Mechanism of Noncatalyzed Hetero-Ene-Reaction (Or Retro-Ene Reaction)[a]

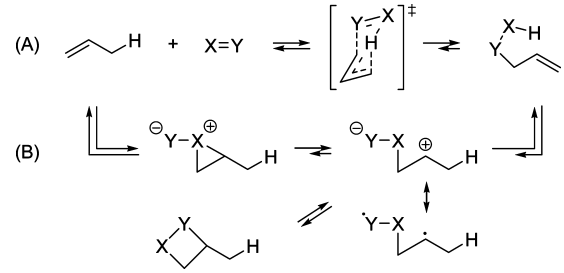

[a] (A) Concerted with six-center transition state: H-transfer is concerted with C−Y bond formation and allylic rearrangement (demonstrated for X = Y: $ArSO_2N$=S=O, SO_2, SeO_2, CO_2, N_2, H_2C=O, H_2C=CH). (B) Nonconcerted involves formation of reactive intermediates in which the H-transfer might not be the rate determining step (observed for X = Y: $^1O_2$, R′CON=NCOR′, TsN=$CHCCl_3$, ArN=O, S=O, SO_3).

Although the ene-reaction of sulfur monoxide (S=O)[23,24] is estimated to have an exothermicity of ca. −28.7 kcal/mol (based on ΔH_f°(S=O, gas) = 1.2 kcal/mol, ΔH_f°(MeSOH, gas) = −45.4 kcal/mol, $\Delta H_f^\circ(CH_4) = -17.9$ kcal/mol,[14] it has never been reported. Sulfur monoxide prefers to undergo cheletropic [2 + 1]-addition with alkenes[25] giving the corresponding thiirane 1-oxides for which no rearrangement into the corresponding product of ene-reaction has been reported yet. This is surprising when comparing with the ene-reaction of singlet oxygen[26−35] and related ene-reactions of diazene derivatives[36−40] and nitroso

(12) King, M. D.; Sue, R. E.; White, R. H.; Young, D. J. *J. Chem. Soc. Chem. Commun.* **1993**, 1797–1798.
(13) Liebman, J. F.; Crawford, K. S. K.; Slayden, S. W. *Supplement S: The Chemistry of Sulphur-Containing Functional Groups*; John Wiley and Sons, Ltd: New York, 1993.
(14) National Institute of Standards and Technology Chemistry WebBook, NT Standard Reference Data-base Number 69; (http://webbook.nist-.gov): Gaithersburg, MD, 2000.
(15) Capozzi, G.; Lucchini, V.; Marcuzzi, F.; Melloni, G. *Tetrahedron Lett.* **1980**, *21*, 3289–3292.
(16) Raasch, M. S.; Smart, B. E. *J. Am. Chem. Soc.* **1979**, *101*, 7733–7734.
(17) Deleris, G.; Kowalski, J.; Dunogues, J.; Calas, R. *Tetrahedron Lett.* **1977**, 4211–4214.
(18) Kresze, G.; Bussas, R. *Liebigs Ann. Chem.* **1980**, 843–857.
(19) Bussas, R.; Kresze, G. *Angew. Chem.* **1980**, *92*, 748–749.
(20) Kresze, G.; Bussas, R. *Angew. Chem.* **1980**, *92*, 750–751.
(21) Deleris, G.; Dunogues, J.; Gadras, A. *Tetrahedron Lett.* **1984**, *25*, 2135–2138.
(22) Starflinger, W.; Kresze, G.; Huss, K. *J. Org. Chem.* **1986**, *51*, 37–40.
(23) Schenk, P. W. *Z. Anorg. Allg. Chem.* **1937**, *233*, 385–400.
(24) Schenk, P. W. *Z. Anorg. Allg. Chem.* **1952**, *270*, 301–303.
(25) Nakayama, J.; Tajima, Y.; Xue-Hua, P.; Sugihara, Y. *J. Am. Chem. Soc.* **2007**, *129*, 7250–7251.
(26) Gollnick, K.; Kuhn, H. *J. Org. Chem.* **1979**, *40*, 287–427.
(27) Stephenson, L. M.; Grdina, M. J.; Orfanopoulos, M. *Acc. Chem. Res.* **1980**, *13*, 419–425.
(28) Davies, A. G.; Schiesser, C. H. *Tetrahedron* **1991**, *47*, 1707–1726.
(29) Singleton, D. A.; Hang, C.; Szymanski, M. J.; Meyer, M. P.; Leach, A. G.; Kuwata, K. T.; Chen, J. S.; Greer, A.; Foote, C. S.; Houk, K. N. *J. Am. Chem. Soc.* **2003**, *125*, 1319–1328.
(30) Maranzana, A.; Ghigo, G.; Tonachini, G. *Chem.—Eur. J.* **2003**, *9*, 2616–2626.
(31) Griesbeck, A. G.; El-Idreesy, T. T.; Adam, W.; rebs, O. *CRC Handbook of Organic Photochemistry and Photobiology*; CRC Press LLC: Boca Raton, FL, 2004; Vol. 8.
(32) Orfanopoulos, M.; Vougioukalakis, G. C.; Stratakis, M. *Chemistry of Peroxides*; John Wiley and Sons, Ltd: Chichester, UK, 2006; Vol. 2. (Pt 2).
(33) Alberti, M. N.; Orfanopoulos, M. *Org. Lett.* **2008**, *10*, 2465–2468.
(34) Leach, A. G.; Houk, K. N.; Foote, C. S. *J. Org. Chem.* **2008**, *73*, 8511–8519.
(35) Sheppard, A. N.; Acevedo, O. *J. Am. Chem. Soc.* **2009**, *131*, 2530–2540.

compounds.[41−47] Exothermicities of ca. −13.4 and −15.6 kcal/mol are estimated for the ene-reactions of triplet dioxygen (based on ΔH_f°(MeOOH) = −31.3 kcal/mol, $\Delta H_f^\circ(CH_4)$ = −17.9 kcal/mol[14]) and diazene (based on ΔH_f°(HN═NH) = 50.9 kcal/mol; ΔH_f°(propane) = −25.0 kcal/mol, $\Delta H_f^\circ(CH_3CH_2CH_2NHNH_2)$ = +11.4 kcal/mol[14]). For the estimate of the heat of ene-reaction of nitroso compounds giving hydroxylamines derivatives (ca. −28 kcal/mol), we have considered the standard heat of hydrogenation $\Delta H_r^\circ(H{-}N{=}O + H_2 \rightarrow H_2NOH)$ = −35.7 kcal/mol[48,49] and compared it with the standard heats of hydrogenation $\Delta H_r^\circ(CH_2O + H_2 \rightarrow MeOH)$ = −21.3 kcal/mol and $\Delta H_r^\circ(CH_2{=}NH + H_2 \rightarrow MeNH_2)$ = −21.6 kcal/mol which are about −8 kcal/mol more exothermic than the corresponding heats of hydrocarbation. Thus, adding to $\Delta H_r^\circ(HNO + H_2 \rightarrow H_2NOH)$ this difference of +8 kcal/mol, we estimate the heat of hydrocarbation of a nitroso compound to amount to ca. −28 kcal/mol (Table 1). In the case of the hydrocarbation of N_2 one estimates a endothermicity of ca. +64.6 kcal/mol (based on $\Delta H_f^\circ(MeCH_2{-}CH_2{-}N{=}NH) = \Delta H_f^\circ(MeCH_2CH_2NHNH_2)$—heat of hydrogenation of azene of −28.1 kcal/mol), and thus, only the retro-ene elimination of N_2 can be observed.[50−52] The ene-reaction of sulfur trioxide (SO_3) is also estimated to be exothermic by ca. −31.4 kcal/mol based on a heat of hydrocarbation of SO_3 of −126 kcal/mol[13] and $\Delta H_f^\circ(SO_3, gas)$ = −94 6 kcal/mol. SO_3 adds to alkenes with high suprafaciality at −60 °C giving the corresponding β-sulfones[53,54] that can be rearranged into the corresponding β,γ-unsaturated sulfonic acids.[55] Related to the ene-reaction of SO_2 is the allylic C−H oxidation with SeO_2[56−58] which occur through an initial ene reaction followed by a [2,3]-sigmatropic shift.[59−61] The ene-reaction follows a concerted process[62] similar to that proposed for **3** → **2** → **1**. After complex formation between SeO_2 and the alkene, direct transfer of the allylic C−H to the O═Se moiety occurs in concert with the C−Se bond formation and the allylic rearrangement. Intermediates such as 1,4-diradical $MeC^{\bullet}H{-}CH_2{-}Se(O){-}O^{\bullet}$ ↔ zwitterion $MeC^{+}HCH_2Se(O)O^{-}$, selenirane 1,1-dioxide (analogous to the [1 + 2]-cheletropic addition of S═O) or 1,2-oxaselenetane 2-oxide (analogous to β-sultones) formed by [2 + 2]-cycloaddition of SeO_2 to alkenes have not been detected[63,64] (Scheme 2).

Although the thermal decarboxylation of but-3-enoic acid into CO_2 and propene is exothermic by ca. +5.3 kcal/mol (based on ΔH_f°(propane) = −25.0 kcal/mol, $\Delta H_f^\circ(CO_2)$ = −94.05 kcal/mol, ΔH_f°(butanoic acid) = −113.7 kcal/mol[14]), and that it is a reaction more exergonic than the desulfinylation of prop-2-ene-1-sulfinic acid, it requires much higher temperatures to occur (>300 °C)[66] than the latter reaction that occurs below 20 °C already in solution. Substituent effects on the activation enthalpy,[67−71] kinetic isotopic effects,[72] as well as quantum calculations[73−77] support a concerted, six-membered mechanism in which the carboxylic hydrogen atom is transferred to C(4) of the but-3-enoic acid in concert with the σ(C(2)−C(1)) bond breaking ($\Delta H^{\ddagger}$ = 38 ± 1.6 kcal/mol, $\Delta S^{\ddagger}$ = −10.2 ± 2.5 e.u. at 377 °C). An analogous reaction is the thermolysis of homoallylic alcohol which fragmentates into propene and formaldehyde above 300 °C ($\Delta H^{\ddagger} \cong$ 40 kcal/mol, $\Delta S^{\ddagger}$ = −8.8 e.u.[78,79] see also the retro-ene reaction of propargyl alcohols[80]) follow a similar concerted mechanism. Thermolysis (287−375 °C) of allyl ethyl ether giving CH_3CHO + propene might also follow a similar concerted retro-ene mechanism,[81,82] as well as thermolysis of allyl methyl amine giving propene + $CH_2{=}NH$ (330−420 °C)[83] (Scheme 2A). Retro-ene elimination of thioaldehydes or thioketones from β,γ-unsaturated thiols is not

(36) Brimble, M. A.; Heathcock, C. H. *J. Org. Chem.* **1993**, *58*, 5261–5263.
(37) Alberti, M. N.; Vougioukalakis, G. C.; Orfanopoulos, M. *Tetrahedron Lett.* **2003**, *44*, 903–905.
(38) Vougioukalakis, G. C.; Roubelakis, M. M.; Alberti, M. N.; Orfanopoulos, M. *Chem.—Eur. J.* **2008**, *14*, 9697–9705.
(39) Roubelakis, M. M.; Vougioukalakis, G. C.; Angelis, Y. S.; Orfanopoulos, M. *Org. Lett.* **2006**, *8*, 39–42.
(40) Lu, X. *Org. Lett.* **2004**, *6*, 2813–2815.
(41) Adam, W.; Bottke, N.; Krebs, O. *J. Am. Chem. Soc.* **2000**, *122*, 6791–6792.
(42) Adam, W.; Bottke, N.; Engels, B.; Krebs, O. *J. Am. Chem. Soc.* **2001**, *123*, 5542–5548.
(43) Leach, A. G.; Houk, K. N. *Chem. Commun.* **2002**, 1243–1255.
(44) Adam, W.; Bottke, N.; Krebs, O.; Lykakis, I.; Orfanopoulos, M.; Stratakis, M. *J. Am. Chem. Soc.* **2002**, *124*, 14403–14409.
(45) Quadrelli, P.; Romano, S.; Piccanello, A.; Caramella, P. *J. Org. Chem.* **2009**, *74*, 2301–2310.
(46) Adam, W.; Krebs, O.; Orfanopoulos, M.; Stratakis, M.; Vougioukalakis, G. C. *J. Org. Chem.* **2003**, *68*, 2420–2425.
(47) Fokin, A. A.; Yurchenko, A. G.; Rodionov, V. N.; Gunchenko, P. A.; Yurchenko, R. I.; Reichenberg, A.; Wiesner, J.; Hintz, M.; Jomaa, H.; Schreiner, P. R. *Org. Lett.* **2007**, *9*, 4379–4382.
(48) Anderson, W. R. *Combust. Flame* **1999**, *117*, 394–403.
(49) Feller, D.; Dixon, D. A. *J. Phys. Chem. A* **2003**, *107*, 10419–10427.
(50) Jabbari, A.; Sorensen, E. J.; Houk, K. N. *Org. Lett.* **2006**, *8*, 3105–3107.
(51) Ripoll, J. L.; Vallee, Y. *Synthesis* **1993**, 659–677.
(52) Mikami, K.; Shimizu, M. *Chem. Rev.* **1992**, *92*, 1021–1050.
(53) Nagayama, M.; Okumura, O.; Noda, S.; Mori, A. *J. Chem. Soc. Chem. Commun.* **1973**, 841.
(54) Morley, J. O.; Roberts, D. W.; Watson, S. P. *J. Chem. Soc. Perkin Trans. 2* **1999**, 1819–1826.
(55) Cerfontain, H.; Kramer, J. B.; Schonk, R. M.; Bakker, B. H. *J. R. Netherlands Chem. Soc.* **1995**, *114*, 410–420.
(56) Dupont, G.; Zacharewicz, W. *Bull. Soc. Chim. Fr.* **1935**, *2*, 533–539.
(57) Guillemonat, A. *Ann. Chem. Fr.* **1939**, *11*, 143–211.
(58) Wiberg, K. B.; Nielsen, S. D. *J. Org. Chem.* **1964**, *29*, 3353–3361.
(59) Sharples, K. B.; Lauer, R. F. *J. Am. Chem. Soc.* **1972**, *94*, 7154–7155.
(60) Arigoni, D.; Vasella, A.; Sharpless, K. B.; Jensen, H. P. *J. Am. Chem. Soc.* **1973**, *95*, 7917–7919.
(61) Woggon, W. D.; Ruther, F.; Egli, H. *J. Chem. Soc. Chem. Commun.* **1980**, 706–708.
(62) Singleton, D. A.; Hang, C. *J. Org. Chem.* **2000**, *65*, 7554–7560.
(63) Ra, C. S.; Park, G. *Tetrahedron Lett.* **2003**, *44*, 1099–1102.
(64) Ra, C. S.; Park, E. M.; Park, G. *Bull. Korean Chem. Soc.* **2008**, *29*, 2513–2516.
(65) Crawford, R. J.; Lutener, S.; Tokunaga, H. *Can. J. Chem.* **1977**, *55*, 3951–3954.
(66) Smith, G. G.; Blau, S. E. *J. Phys. Chem.* **1964**, *68*, 1231–1234.
(67) Bigley, D. B. *J. Chem. Soc.* **1964**, 3897–3899.
(68) Noyce, D. S.; Heller, R. A. *J. Am. Chem. Soc.* **1965**, *87*, 4325–4328.
(69) Bigley, D. B.; Thurman, J. C. *J. Chem. Soc.* **1965**, 6202–6205.
(70) Bigley, D. B.; Thurman, J. C. *J. Chem. Soc. B: Phys. Org.* **1966**, 1076–1077.
(71) Bigley, D. B.; May, R. W. *J. Chem. Soc. B: Phys. Org.* **1967**, 557–560.
(72) Bigley, D. B.; Thurman, J. C. *J. Chem. Soc. B: Phys. Org.* **1967**, 941–943.
(73) Dewar, M. J. S.; Ford, G. P. *J. Am. Chem. Soc.* **1977**, *99*, 8343–8344.
(74) Lee, I.; Cho, J. K. *Bull. Korean Chem. Soc.* **1984**, *5*, 51–52.
(75) Lee, I.; Cho, J. K.; Lee, B. S. *J. Comput. Chem.* **1984**, *5*, 217–224.
(76) Wang, Y. L.; Poirier, R. A. *Can. J. Chem.* **1994**, *72*, 1338–1346.
(77) Dunn, M. E.; Shields, G. C.; Takahashi, K.; Skodje, R. T.; Vaida, V. *J. Phys. Chem. A* **2008**, *112*, 10226–10235.
(78) Smith, G. G.; Yates, B. L. *J. Chem. Soc.* **1965**, 7242–7246.
(79) Inaba, T.; Sakamoto, M.; Watanabe, S.; Takahashi, I.; Fujita, T. *J. Chem. Technol. Biotechnol.* **1990**, *48*, 483–492.
(80) Hopf, H.; Kirsch, R. *Angew. Chem.* **1985**, *24*, 796–797.
(81) Egger, K. W.; Vitins, P. *Int. J. Chem. Kinet.* **1974**, *6*, 429–435.
(82) Vitins, P.; Egger, K. W. *J. Chem. Soc. Perkin Trans. 2* **1974**, 1292–1293.
(83) Vitins, P.; Egger, K. W. *J. Chem. Soc. Perkin Trans. 2* **1974**, 1289–1291.

Scheme 3. One-Pot Synthesis of Stereotriads via SO_2−Umpolung

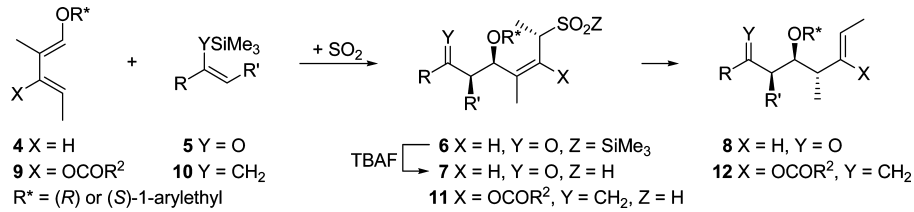

described, but examples of ene-reaction of thiocarbonyl compounds are known.[84,85]

As stated above, β,γ-unsaturated sulfinic acids are unstable at room temperature. They are formed as intermediates in the hydrolysis of sulfinamides,[5,6,8−11] the reduction of β-ketosulfones,[86] and the oxidation of allylic thiols.[87] They have been proposed as intermediates in SO_2-mediated alkene isomerization.[1,16,88−90] As we have shown, this might not always be true.[91] In the case of 1,1-dialkylethenes and trialkyl substituted alkenes, SO_2 generates first polysulfone polymers with the alkenes. The latter are responsible for hydrogen atom abstraction from the alkenes and generate allyl radical intermediates that finally provide the most stable alkene isomers.[92]

In 1997, our group uncovered a new C−C bond-forming reaction cascade that condenses butadien-1-yl ethers **4**, enoxysilanes **5** and SO_2 to generate β,γ-unsaturated silyl sulfinates **6**. After desilylation, the corresponding sulfinic acid **7** undergo SO_2 elimination with formation of (*E*)-alkenes **8** with high stereoselectivity.[93] The reaction cascade has been applied to several diene(**4**)/enoxysilane(**5**) pairs,[94−97] as well as to diene(**9**)/allylsilane(**10**) pairs[98] (Scheme 3), thus giving us the possibility to construct, in one-pot operations, stereotriads **8** and **12** that can be used directly in the synthesis of long-chain polyketides and polypropionates.[99,100] In some cases, the desulfinylations, which require acidic conditions, are accompanied by decomposition of the desired polyfunctional products. To avoid this, we have been forced to study the mechanism of the desulfinylation of β,γ-unsaturated sulfinic acid in more detail with the goal to find suitable reaction conditions under which undesired side-reactions such as R*OH elimination and retro-aldol cleavage would be suppressed. An alternative route is the Pd-catalyzed desulfinylation of silyl β,γ-unsaturated sulfinates.[101]

As we had found that SO_2 catalyzes its hetero-Diels−Alder and cheletropic additions,[102−104] we hoped that it would also catalyze the desulfinylation of β,γ-unsaturated sulfinic acid under less acidic conditions than protic or Lewis acid. We thus have investigated the kinetics of the desulfinylation of prop-2-enesulfinic acid (**13**) under various conditions. As the reaction in toluene is quick at room temperature,[4,12] we decided to work at −15 °C in CD_2Cl_2, using ^1H NMR to follow the reactions. As we shall see, and in contrast to the studies reported by Young and co-workers,[4] the rate laws are more complicated than first order in sulfinic acid. We also find that CF_3COOH does not catalyze the reactions much better than sulfinic **13** acid itself. To our surprise SO_2 has no significant effect on the rate of the desulfinylation of **13**. At low concentration, $BF_3 \cdot Et_2O$ has no significant effect, whereas at high concentration, it inhibits the reaction, in contrast with the efficient catalytical effect of $BF_3 \cdot Et_2O$,[105−108] on related carbonyl-ene reactions.[3,109−117]

In parallel with these kinetics, we have carried out extensive quantum calculations to approach a better understanding of our observations and to delimit the possible mechanisms of the retro-ene reaction (Schemes 1 and 2). This led us to find various transition structures and paths for the desulfinylations. The favored transition structures for uncatalyzed and "catalyzed" reactions involve chairlike structures H atom transfer from C−H to O═S occurs in concert with the C−S bond formation, in which the S═O bond of the sulfinyl group not involved in the

(84) Motoki, S.; Watanabe, T.; Saito, T. *Tetrahedron Lett.* **1989**, *30*, 189–192.
(85) El-Sayed, I.; Franek, W.; Abdel-Megeed, M. F.; Yassin, S. M.; Gylling, A.; Senning, A. *Sulfur Lett.* **1995**, *19*, 59–66.
(86) Baldwin, J. E.; Adlington, R. M.; Ichikawa, Y.; Kneale, C. J. *J. Chem. Soc. Chem. Commun.* **1988**, 702–704.
(87) Engler, T. A.; Ali, M. H.; Vander Velde, D. *Tetrahedron Lett.* **1989**, *30*, 1761–1764.
(88) Rogic, M. M.; Masilamani, D. *J. Am. Chem. Soc.* **1977**, *99*, 5219–5220.
(89) Masilamani, D.; Rogic, M. M. *J. Am. Chem. Soc.* **1978**, *100*, 4634–4635.
(90) Masilamani, D.; Reuman, M. E.; Rogic, M. M. *J. Org. Chem.* **1980**, *45*, 4602–4605.
(91) Markovic, D.; Vogel, P. *Angew. Chem., Int. Ed.* **2004**, *43*, 2928–2930.
(92) Markovic, D.; Varela-Alvarez, A.; Sordo, J. A.; Vogel, P. *J. Am. Chem. Soc.* **2006**, *128*, 7782–7795.
(93) Deguin, B.; Roulet, J. M.; Vogel, P. *Tetrahedron Lett.* **1997**, *38*, 6197–6200.
(94) Roulet, J. M.; Puhr, G.; Vogel, P. *Tetrahedron Lett.* **1997**, *38*, 6201–6204.
(95) Turks, M.; Murcia, M. C.; Scopelliti, R.; Vogel, P. *Org. Lett.* **2004**, *6*, 3031–3034.
(96) Turks, M.; Huang, X. G.; Vogel, P. *Chem.—Eur. J.* **2005**, *11*, 465–476.
(97) Craita, C.; Didier, C.; Vogel, P. *Chem. Commun.* **2007**, 2411–2413.
(98) Turks, M.; Fonquerne, F.; Vogel, P. *Org. Lett.* **2004**, *6*, 1053–1056.
(99) Vogel, P.; Turks, M.; Bouchez, L. C.; Markovic, D.; Varela-Alvarez, A.; Sordo, J. A. *Acc. Chem. Res.* **2007**, *40*, 931–942.
(100) Vogel, P.; Turks, M.; Bouchez, L.; Craita, C.; Huang, X. G.; Murcia, M. C.; Fonquerne, F.; Didier, C.; Flowers, C. *Pure Appl. Chem.* **2008**, *80*, 791–805.
(101) Huang, X. G.; Craita, C.; Vogel, P. *J. Org. Chem.* **2004**, *69*, 4272–4275.
(102) Fernandez, T.; Sordo, J. A.; Monnat, F.; Deguin, B.; Vogel, P. *J. Am. Chem. Soc.* **1998**, *120*, 13276–13277.
(103) Monnat, F.; Vogel, P.; Rayon, V. M.; Sordo, J. A. *J. Org. Chem.* **2002**, *67*, 1882–1889.
(104) Monnat, F.; Vogel, P.; Meana, R.; Sordo, J. A. *Angew. Chem., Int. Ed.* **2003**, *42*, 3924–3927.
(105) Maruoka, K.; Ooi, T.; Yamamoto, H. *J. Am. Chem. Soc.* **1990**, *112*, 9011–9012.
(106) Achmatowicz, O.; Szechner, B. *J. Org. Chem.* **1972**, *37*, 964–967.
(107) Okachi, T.; Fujimoto, K.; Onaka, M. *Org. Lett.* **2002**, *4*, 1667–1669.
(108) Okachi, T.; Onaka, M. *Stud. Surf. Sci. Catal.* **2003**, *145*, 141–144.
(109) Oppolzer, W.; Snieckus, V. *Angew. Chem., Int. Ed. Engl.* **1978**, *17*, 476–486.
(110) Snider, B. B. *Acc. Chem. Res.* **1980**, *13*, 426–432.
(111) Song, Z. G.; Beak, P. *J. Am. Chem. Soc.* **1990**, *112*, 8126–8134.
(112) Achmatowicz, O.; Bialecka-Florjanczyk, E. *Tetrahedron* **1996**, *52*, 8827–8834.
(113) Braddock, D. C.; Hii, K. K. M.; Brown, J. M. *Angew. Chem., Int. Ed.* **1998**, *37*, 1720–1723.
(114) Yamanaka, M.; Mikami, K. *Helv. Chim. Acta* **2002**, *85*, 4264–4271.
(115) Morao, M.; McNamara, J. P.; Hillier, A. H. *J. Am. Chem. Soc.* **2003**, *125*, 628–629.
(116) Choomwattana, S.; Maihom, T.; Khongpracha, P.; Probst, M.; Limtrakul, J. *J. Phys. Chem. C* **2008**, *112*, 10855–10861.
(117) Clarke, M. L.; France, M. B. *Tetrahedron* **2008**, *64*, 9003–9031.

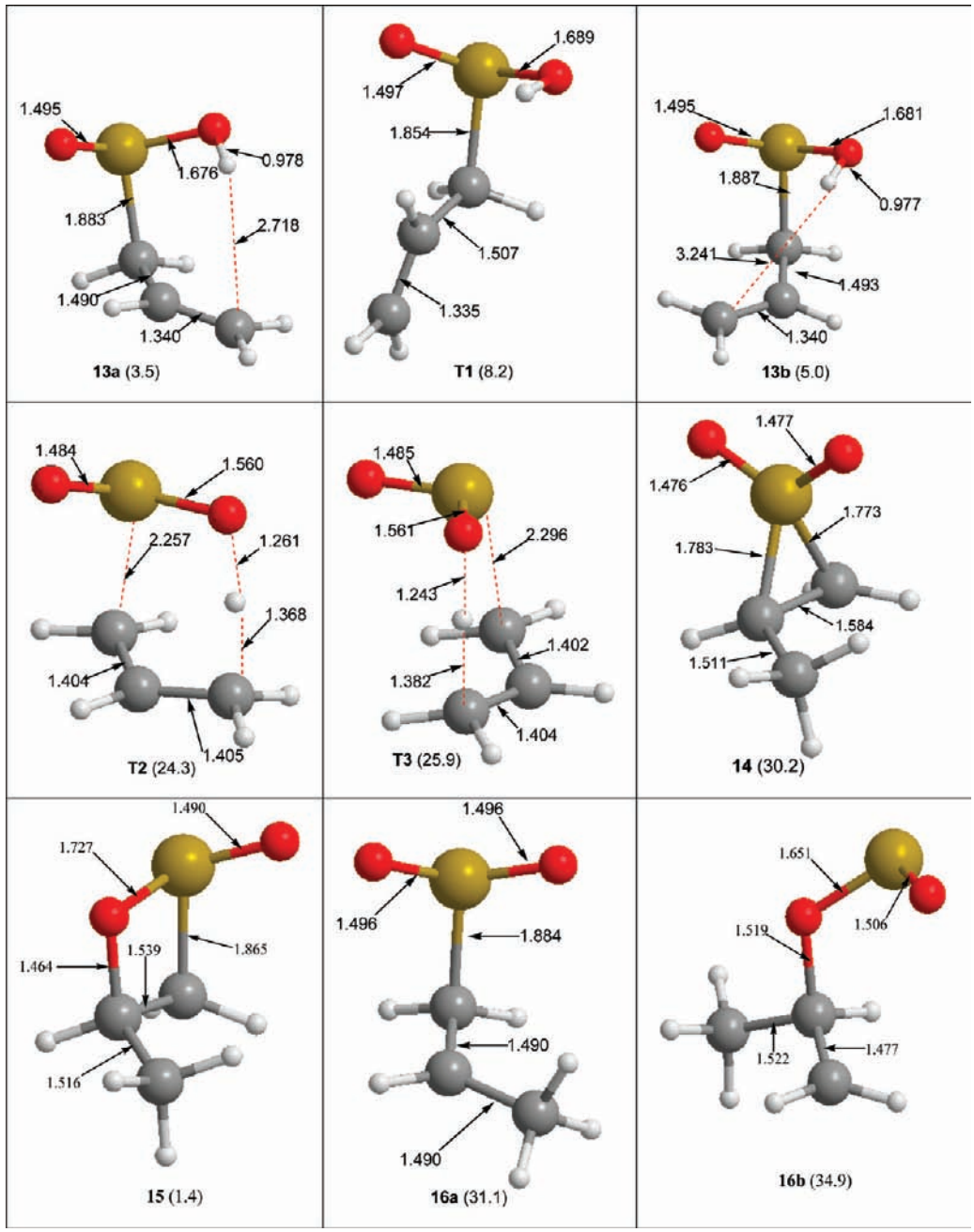

Figure 1. B3LYP/6-31+G(d,p) structures of the species located on the PES of the retro-ene reaction of monomeric prop-2-enesulfinic acid (**13**). In parentheses, CCSD(T)/6-311+G(d,p)//B3LYP//6-31+G(d,p) Gibbs free energy differences, including solvent effects, with respect to $0.5\cdot(\mathbf{13})_2$ (Table 2).

pericyclic reaction occupies pseudoaxial position which prefers to be gauche with respect to the C(1)−C(2) bond. This stabilizing gauche effect is also found in prop-2-ene sulfinic acid itself and in its dimer that forms in CH_2Cl_2 at −15 °C. Thus, our calculations have uncovered a case of stabilizing gauche effect that involves a polar S═O bond and a much less polar C−C bond. Other possible mechanisms involving the intermediacy of β-sultane, thirane-1,1-dioxide or 1,4-diradical ↔ zwitterionic intermediates require higher activation free energies than the concerted mechanism.

Theoretical Methods

Geometry optimizations were carried out using density functional theory (DFT)[118] with the Becke three-parameter Lee−Yang−Parr[119,120] (B3LYP) hybrid functional and Pople's 6-31+G(d,p) basis set.[121] All the geometrical parameters were fully optimized, and all the structures located on the potential energy surfaces (PESs) were characterized as minima or transition structures by computing the corresponding Hessian matrices and examining the number of imaginary frequencies from them. Graphical analysis of the imaginary frequencies of the transition structures, as well as intrinsic reaction coordinate

(118) Koch, W.; Holthausen, M. C. *A Chemist's Guide to Density Functional Theory*, 2nd ed.; Wiley-VCH: Weinheim, 2000.
(119) Lee, C. T.; Yang, W. T.; Parr, R. G. *Phys. Rev. B* **1988**, *37*, 785–789.
(120) Becke, A. D. *J. Chem. Phys.* **1993**, *98*, 5648–5652.
(121) Hehre, W. J.; Radom, L.; Schleyer, P. v. R.; Pople, J. A. *Ab initio Molecular Orbital Theory*; Wiley: New York, 1986.

(IRC) calculations, allowed us to interconnect the different structures located on the PESs and then construct the corresponding energy profiles.

The energy predictions were improved by performing single-point CCSD(T)/6-311+G(d,p)//B3LYP/6-31+G(d,p) calculations.[121,122] Solvent effects were estimated through quantum mechanical free energy calculations based on the self-consistent reaction field (SCRF) method augmented by atomic surface tensions.[123] The so-called solvation model 5.43 (SM5.43R)[124,125] was employed. This model is specially suitable in the present case as it was parametrized to predict the free energy of solvation of solutions with species containing H, C, O, and S atoms in organic solvents (including CH_2Cl_2) using B3LYP/6-31G(d) method to describe the electronic structure of the solute. Calculations were carried out for CH_2Cl_2 as a solvent, thus simulating experimental conditions. The ion convention standard state (1M)[122] was used to compute the changes in Gibbs free energies.

The thermodynamic functions (ΔH, ΔS, and ΔG) were estimated within the ideal gas, rigid rotor, and harmonic oscillator approximations.[126] A temperature of 258.15 K was assumed. Kinetics calculations were performed within the context of the conventional transition state theory (CTST),[127] estimating tunnel effects by means of the small curvature tunnelling (SCT) approximation.[128] The Gaussian03 package of programs[129] was used to carry out the electronic structure calculations.

Results and Discussion

Quantum Calculations. In a first series of calculations, we examined the PES of prop-2-enesulfinic acid (**13**) without any additive. As expected for sulfinic acids in solution,[130−133] dimers exist in equilibrium with the monomeric acids due to favorable S=O···H−OS hydrogen bonding. In the case of **13** + **13** ⇄ $(\mathbf{13})_2$ (Figure 2 and Table 2), we calculate for CH_2Cl_2 solution at −15 °C $\Delta G = -3.5$ kcal/mol, or $K(\mathbf{13} + \mathbf{13} \rightleftarrows (\mathbf{13})_2) = 919$. Interestingly, both molecules of **13** in dimer $(\mathbf{13})_2$ adopt the same privileged conformation shown in Scheme 3 in which the S=O and σ(C(1)−C(2)) bond are gauche, the C−H bond at C(2) pointing toward the oxygen center of S=O. The S−OH moiety is antiperiplanar with respect to σ(C(1)−C(2)).

Two conformers are found for monomeric **13**. In both of them, **13a** and **13b**, S=O/σ(C(1)−C(2)) and S−OH/σ(C(1)−C(2)) are gauche. Monomers **13a** and **13b** are equilibrated by rotation about the σ(C(1)−C(2)) bond through transition state **T1** (Figure 1). The greater stability of **13a** with respect to **13b** (1.5 kcal/mol) might be attributed to hydrogen bridging between the SOH group and the π-electrons of the alkene unit that is more favorable in **13a** than in **13b** (Table 2).

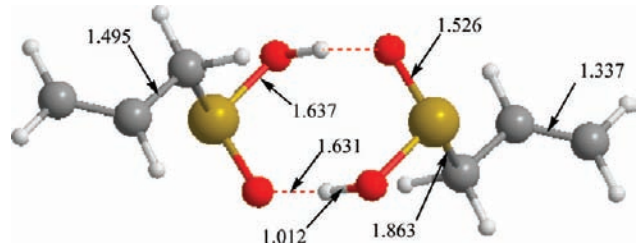

Figure 2. B3LYP/6-31G+G(d,p) structure for the $(\mathbf{13})_2$ dimer.

Table 2. CCSD(T)/6-311+G(d,p)//B3LYP//6-31+ G(d,p) Relative Energy Values for the Intermediates and Transition Structures of the Monomolecular and Bimolecular Mechanisms of the Retro-Ene Elimination of SO_2 from Prop-2-enesulfinyl Acid (**13**)[a]

structure		ΔU	ΔH	ΔS	ΔG	$\Delta G_{solv,SMX}$
dimer	$0.5\cdot(\mathbf{13})_2$	0.0	0.0	0.0	0.0	0.0
monomer	**13a**	11.7	11.1	19.2	6.9	3.5
	T1	16.8	15.3	17.9	11.4	8.2
	13b	13.0	12.4	20.5	7.9	5.0
monomolecular	**T2**	35.6	31.6	15.1	28.5	24.3
	T3	37.2	33.1	15.4	29.9	25.9
bimolecular	**T4**	31.7	28.6	0.9	28.4	25.8
	T5	33.8	30.5	0.4	30.4	28.4
Propene + SO_2		11.6	9.0	57.0	−3.4	−5.6

[a] ΔU, ΔH, and ΔS are calculated at 258.15 K and 1 atm. ΔG and $\Delta G_{solv,SMX}$ calculated using standard state (1 M, 258.15 K).[122] All energy values are given in kcal/mol, entropies (ΔS) in cal/K·mol.

Scheme 4

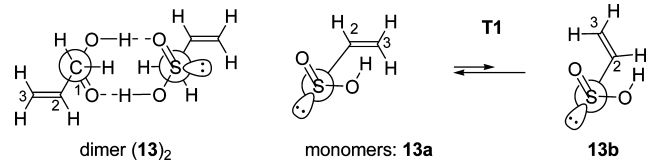

As found experimentally (sealed tube experiments), the conversion of $(\mathbf{13})_2$ into **13** + propene + SO_2 is exergonic at −15 °C. Monomer **13a** undergoes retro-ene elimination of SO_2 following a one-step, concerted mechanism for which transition structure **T2** is located (Figures 1 and 3, Table 2) and which shows a C−S bond significantly elongated (from 1.833 Å in **13a** to 2.257 Å in **T2**) and a high degree of C(3)−H bond formation (from 2.748 Å in **13a** to 1.382 Å in **T2**). In **T2**, S=O and σ(C(1)−C(2)) are gauche, as in **13a**. This transition structure realizes a six-membered ring with H−C(1) bonds both staggered with S−O, and S=O bonds (Scheme 5). Furthermore, if one considers the plane realized by S, C(1), and C(3), the oxygen center of S−OH is below this plane whereas C(2) is above this plane, making it to resemble a chair type of structure with an axial S=O group. Our calculations predict a second transition state for the retro-ene elimination of SO_2 from monomeric **13** which is 1.6 kcal/mol higher in free energy than **T2**. Such a transition structure, **T3**, adopts a conformation resembling that of a boat six-membered ring in which S−O and σ(C(1)−C(2)) bonds, as well as one of the two C(1)−H bonds and S=O double bond, are nearly eclipsed. These eclipsing interactions are avoided in **T2**, thus explaining the lower free energy of **T2** compared with **T3** (Table 2). Scheme 5 shows the two possible reaction pathways for the monomolecular retro-ene mechanism.

(122) Cramer, C. J. *Essentials of Computational Chemistry: Theories and Models*; Wiley: Chichester, 2002.
(123) Chamberlin, A. C.; Kelly, C. P.; Thompson, J. D.; Lynch, B. J.; Xidos, J. D.; Hawkins, G. D.; Li, J.; Zhu, T. H.; Volobuev, Y.; Rinaldi, D.; Liotard, D. A.; Cramer, C. J.; Truhlar, D. G. *SMXGAUS, version 3.4.2*; University of Minnesota: Minneapolis, 2007.
(124) Thompson, J. D.; Cramer, C. J.; Truhlar, D. G. *J. Phys. Chem. A* **2004**, *108*, 6532–6542.
(125) Thompson, J. D.; Cramer, C. J.; Truhlar, D. G. *Theor. Chem. Acc.* **2005**, *113*, 107–131.
(126) McQuarrie, D. A. *Statistical Thermodynamics*; University Science Books: Mill Valley, CA, 1973.
(127) Laidler, K. J. *Chemical Kinetics*; Harper and Row: New York, 1987.
(128) Fernandez-Ramos, A.; Miller, J. A.; Klippenstein, S. J.; Truhlar, D. G. *Chem. Rev.* **2006**, *106*, 4518–4584.
(129) Frisch, M. J.; *Gaussian03, Revision C.01*; Gaussian, Inc.: Wallington, CT, 2004.
(130) Wright, W. G. *J. Chem. Soc.* **1949**, 683–692.
(131) Wudl, F.; Lightner, D. A.; Cram, D. J. *J. Am. Chem. Soc.* **1967**, *89*, 4099–4101.
(132) Minkwitz, R.; Kornath, A.; Lohmann, U. *Z. Naturforsch. Teil B* **1996**, *51*, 739–743.

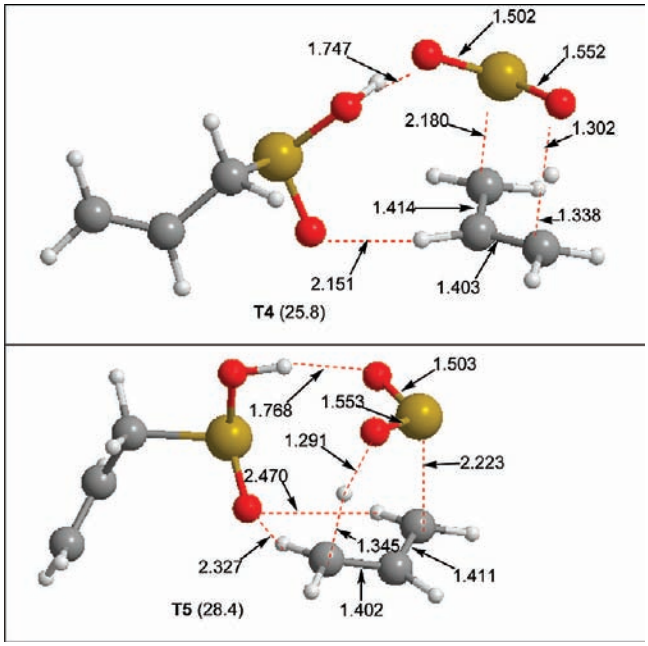

Figure 3. B3LYP/6-31+G(d,p) structures of the species located on the PES of the retro-ene reaction of prop-2-enesulfinic acid (**13**) in the presence of a second molecule of **13**. Some selected bond distances are given in Å. In parentheses, CCSD(T)/6-311+G(d,p)//B3LYP//6-31+G(d,p) Gibbs free energy differences, including solvent effects, with respect to 0.5·(**13**)$_2$ (Table 3).

Scheme 5

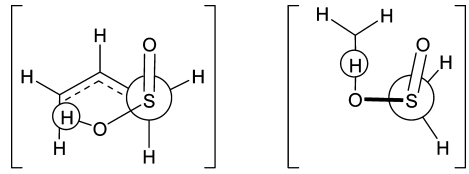

It should be mentioned that a weak complex between SO_2 and propene was located on the PES. However, it resulted higher in Gibbs free energy than products (SO_2 + propene) and, consequently, it has been not included in the ΔG profile shown in Scheme 6.

For the ene-reactions of alkenes with singlet dioxygen,[29,33,43,134] with nitrosoarenes,[42,43,46,135,136] triazolinediones,[39,46,137−143] and aldehydes[3,111−114,116] mechanisms involving intermediates have been invoked in some cases. Interestingly, Houk, Singleton, and co-workers[29] and Singleton and co-workers[144] have shown theoretical evidence supporting the possibility of a two-step no-intermediate mechanism for some particular ene reactions as a direct consequence of the presence of valley−ridge inflections on their PESs. Indeed, the existence of the so-called branching points (those having all vibrational frequencies positive but one being zero)[145,146] has been shown to be crucial in order to rationalize fundamental aspects of chemical reactivity[29,144,147] and weak interactions.[148,149] We have explored the possibility of existence of some thiirane 1-dioxide **14**, β-sultane **15**, or diradical intermediates **16a**, **16b** (see Figure 1 and Scheme 7) on the PES for the retro-ene reaction of **13**. Figure 1 shows the four structures we located as intermediates at the B3LYP/6-31+G(d,p) level. Their corresponding CCSD(T)/6-311+G(d,p)//B3LYP/6-31+G(d,p) Gibbs free energies, including solvent effects, become 30.2, 1.4, 34.2, and 34.9 kcal/mol, respectively. Therefore, participation of the 1-dioxide **14** and diradical intermediates **16a**, **16b** in the retro-ene elimination mechanism is unlikely. The β-sultane **15**, resulting from a formal [2 + 2]-cycloaddition, is slightly less stable than sulfinic acid **13**. As expected,[150−152] a concerted mechanism involves a rather high energy transition state (37.5 kcal/mol). A two-step process would imply diradical structures **16a**, **16b**; both also are too high in free energy. As a conclusion, our calculations suggest the monomolecular retro-ene elimination of SO_2 from prop-2-enesulfinic acid to proceed through a concerted, pericyclic pathway.

In a second series of calculations we examined whether dimer (**13**)$_2$ (Figure 2) would be able to undergo the retro-ene elimination of SO_2 without monomerization, thus involving "autocatalysis" of the ene reaction. Transition structures **T4** ($\Delta G^{\ddagger}$ = 25.4 kcal/mol) and **T5** ($\Delta G^{\ddagger}$ = 28.4 kcal/mol) (Figure 3, Table 2) correspond to the lowest free energy transition states calculated for bimolecular mechanisms. The data suggest that a bimolecular mechanism, at least through transition state **T4**, can compete at −15 °C with the monomolecular retro-ene reactions involving transition states **T2** and **T3**, as observed experimentally (see below). Transition structures **T4** and **T5** can be formally viewed as transition structures **T2** and **T3**, respectively, stabilized by a hydrogen bonding between their S=O moieties and the corresponding SOH groups of the spectrator molecule **13**. There are also weaker electrostatic interactions involving the S=O moiety of spectrator molecule **13** and the C−H bond at C(2) in **T2** or the C−H bond at C(1) and C(3) in **T3**. These interactions represent favorable enthalpic effects as can be seen in Table 1: $\Delta H^{\ddagger}$ (**T2**) = 31.6 kcal/mol vs $\Delta H^{\ddagger}$ (**T4**) = 28.6 kcal/mol. However, entropic contributions clearly favor **T2**: $\Delta G_{solv,SMX}{}^{\ddagger}$ (**T2**) = 24.3 kcal/mol vs $\Delta G_{solv,SMX}{}^{\ddagger}$ (**T4**) = 25.8 kcal/mol.

It is well known that consideration of transition structures involving additional molecules of one of the reactants acting

(133) Beckmann, J.; Finke, P.; Hesse, M.; Wettig, B. *Angew. Chem., Int. Ed.* **2008**, *47*, 9982–9984.
(134) Orfanopoulos, M. *Mol. Supramol. Photochem.* **2001**, *8*, 243–285.
(135) Adam, W.; Krebs, O.; Orfanopoulos, M.; Stratakis, M. *J. Org. Chem.* **2002**, *67*, 8395–8399.
(136) Leach, A. G.; Houk, K. N. *Org. Biomol. Chem.* **2003**, *1*, 1389–1403.
(137) Ohashi, S.; Butler, G. B. *J. Org. Chem.* **1980**, *45*, 3472–3476.
(138) Seymour, C. A.; Greene, F. D. *J. Am. Chem. Soc.* **1980**, *102*, 6384–6385.
(139) Cheng, C. C.; Seymour, C. A.; Petti, M. A.; Greene, F. D.; Blount, J. F. *J. Org. Chem.* **1984**, *49*, 2910–2916.
(140) Elemes, Y.; Foote, C. S. *J. Am. Chem. Soc.* **1992**, *114*, 6044–6050.
(141) Chen, J. S.; Houk, K. N.; Foote, C. S. *J. Am. Chem. Soc.* **1997**, *119*, 9852–9855.
(142) Singleton, D. A.; Hang, C. *J. Am. Chem. Soc.* **1999**, *121*, 11885–11893.
(143) Acevedo, O.; Squillacote, M. E. *J. Org. Chem.* **2008**, *73*, 912–922.
(144) Bekele, T.; Christian, C. F.; Lipton, M. A.; Singleton, D. A. *J. Am. Chem. Soc.* **2005**, *127*, 9216–9223.
(145) Bosch, E.; Moreno, M.; Lluch, J. M.; Bertran, J. *Chem. Phys. Lett.* **1985**, *160*, 543–548.
(146) Quapp, W.; Heidrich, D. *J. Mol. Struct. (THEOCHEM)* **2002**, *585*, 105–117.
(147) Brana, P.; Menendez, B.; Fernandez, T.; Sordo, J. A. *J. Phys. Chem. A* **2000**, *104*, 10842–10854.
(148) Valdes, H.; Rayon, V. M.; Sordo, J. A. *Chem. Phys. Lett.* **1999**, *309*, 265–273.
(149) Valdes, H.; Sordo, J. A. *Chem. Phys. Lett.* **2001**, *333*, 169–180.
(150) Sordo, J. A.; González, J.; Sordo, T. L. *J. Am. Chem. Soc.* **1992**, *114*, 6249–6251.
(151) Assfeld, X.; Ruiz-López, M. F.; González, J.; López, R.; Sordo, J. A.; Sordo, T. L. *J. Comput. Chem.* **1994**, *15*, 479–487.
(152) Braña, P.; Gimeno, J.; Sordo, J. A. *J. Org. Chem.* **2004**, *69*, 2544–2550.

Scheme 6. CCSD(T)/6-31+G(d,p)//B3LYP/6-31+G(d,p) + SM5.43R ΔG Profile

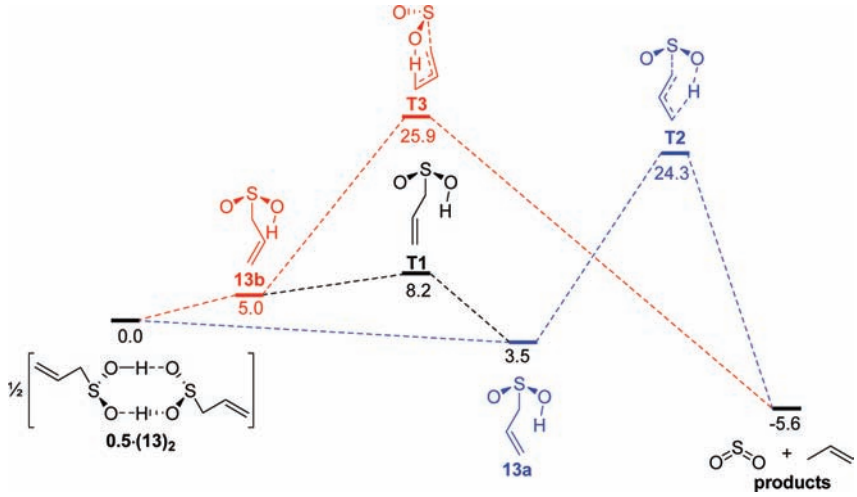

Table 3. CCSD(T)/6-311+G(d,p)//B3LYP/6-31+G(d,p) Relative Energy Values for the Intermediates and Transition Structures of the Retro-Ene Reaction of **13** in the Presence of Additive A (SO_2, BF_3, CF_3COOH)[a]

Structure	ΔU	ΔH	ΔS	ΔG	$\Delta G_{solv,SMX}$	
0.5·(**13**)$_2$ + A	(0.0)	(0.0)	(0.0)	(0.0)	(0.0)	
13a + A	11.7	11.1	19.2	6.9	3.5	
13b + A	13.0	12.4	20.5	7.9	5.0	
T6 (A = SO_2)	26.0	23.2	14.4	26.1	25.2	
T7 (A= SO_2)	27.7	24.8	-16.2	28.2	27.5	
16 (A = BF_3)	-8.6	-8.3	-21.3	-3.5	-11.2	
17 (A = BF_3)	-4.5	-4.2	-17.4	-0.5	-9.8	
0.5·18 (A = BF_3)	-21.4	-20.4	-39.0	-11.9	-15.5	$\Delta G^{\ddagger} = 23.8$
T8 (A = BF_3)	16.9	14.0	-24.8	19.6	8.3	
T9 (A = BF_3)	21.8	18.7	-22.4	23.7	12.3	
T10 (A = CF_3COOH)	20.9	18.1	-18.7	22.2	23.2	
T11 (A = CF_3COOH)	21.0	18.1	-20.1	22.5	24.0	
Propene + SO_2+ A	11.6	9.0	57.0	-3.4	-5.6	

[a] ΔU, ΔH, and ΔS calculated at 258.15 K and 1 atm. ΔG and $\Delta G_{solv,SMX}$ calculated using the standard state 1 M at 258.15 K.[122] All energy values are given in kcal/mol, entropies (ΔS) in cal/K·mol.

Scheme 7

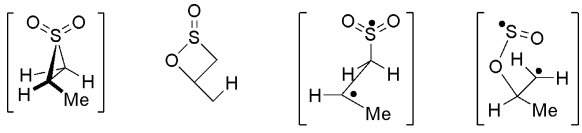

as a catalyst can sometimes be relevant.[153] As previous studies on the hetero-Diels−Alder and cheletropic addition of sulfur dioxide had shown that SO_2 promotes these reactions,[102,103,154] we examined whether this could also be the case for the ene-reaction of SO_2 with propene. Our results are summarized in Table 3 for the lowest possible transition states **T6** and **T7** (Figure 4). Formally, on approaching transition structure **T2** as in **T6**, one molecule of SO_2 interacts with the S═O moiety of **T2** through its S center. There is also a weak electrostatic interaction between one S═O moiety of SO_2 and C−H at C(2). In the case of SO_2 approaching **T3**, as in **T7**, again the S═O moiety of **T3** interacts with the S center of SO_2 and a weak electrostatic interaction can be recognized between one S═O moiety of SO_2 with C−Hs at C(1) and C(3) of **T3**. Comparison of the differences of enthalpies (ΔH, Tables 2 and 3) calculated for **T6** (23.2 kcal/mol)/**T2** (31.6 kcal/mol) and **T7** (24.8 kcal/mol)/**T3** (33.1 kcal/mol) one finds that SO_2 stabilizes both transition structures **T2** and **T3**. Nevertheless, because of the negative entropy this requires, the calculated free energy of activation are higher at −15 °C for the SO_2-assisted reactions (25.2 and 27.5 kcal/mol) than for the monomolecular retro-ene reactions (24.3 and 25.9 kcal/mol). This prediction is confirmed experimentally (see Table 4).

Lewis acids promote the hetero-Diels−Alder and cheletropic additions of SO_2.[155,156] We thus examined the effect of BF_3 on the desulfinylation of **13**. Experiments were carried out using both BF_3 and BF_3·Me_2O moieties. We focused our theoretical analysis on the reaction in the presence of BF_3 to keep the computational cost within reasonable limits. Some comments on the stability of **19** when employing BF_3·Me_2O can be found in Section D. Calculations show that both conformers of **13** form stable complexes **17** (BF_3 + **13a**) and **18** (BF_3 + **13b**). Interestingly, dimer (**13**)$_2$ combines with 2 equiv of BF_3 forming tetramolecular complex **19** (Figure 5). In CH_2Cl_2 at −15 °C complexes **17** (−11.2 kcal/mol), **18** (−9.8 kcal/mol), and **19** (−15.5 kcal/mol) are definitively more stable than BF_3 + 0.5·

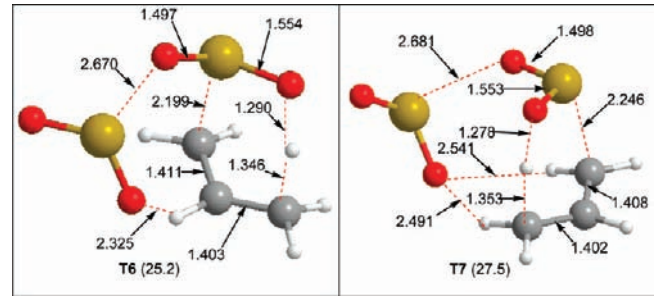

Figure 4. B3LYP/6-31+G(d,p) structures of the transition states located on the PES of the retro-ene reaction of **13** in the presence one molecule of SO_2. Some selected bond distances are given in Å. In parentheses, CCSD(T)/6-311+G(d,p)//B3LYP//6-31+G(d,p) Gibbs free energy differences, including solvent effects, with respect to 0.5·(**13**)$_2$ (Table 3).

(153) Menéndez, M. I.; Suarez, D.; Sordo, J. A.; Sordo, T. L. *J. Comput. Chem.* **1995**, *16*, 659–666.
(154) Vogel, P.; Sordo, J. A. *Curr. Org. Chem.* **2006**, *10*, 2007–2036.
(155) Deguin, B.; Vogel, P. *J. Am. Chem. Soc.* **1992**, *114*, 9210–9211.

Table 4. Experimental Kinetic Data Obtained for the Desulfinylation of **13**[a] in CD_2Cl_2 at −15 °C[b]

entry	*n*(TFA)/*n*(tin sulf)	additive (other conditions)	k'/min^{-1}	k''/(mol$^{1/2}$/kg$^{1/2}$·min)
1	0.47	−	0.00575	
2	0.86	−	0.00565	
3	1.19	TFA (0.19 equiv)	0.00578	0.00231
4	1.88	TFA (0.88 equiv)	0.00564	0.00335
5	5.60	TFA (4.6 equiv)	0.0055	0.00928
6	0.89	BF_3 OMe_2, (0.19 equiv)	0.0061	0.00065
7	0.82	BF_3 OMe_2, (10 equiv)	no reaction	
8	0.73	TBAF (0.26 equiv)	0.00581	0.00004
9	0.83	SO_2 (12.99 equiv)	0.0063	0.00099
10	0.92	C_6D_{12}, 25 °C	0.02927	
11	0.80	CD_2Cl_2, 25 °C	too fast to be measured by NMR	

[a] Prepared by addition of CF_3COOH (TFA) solution in CD_2Cl_2 to a CD_2Cl_2 solution of tributyltin prop-2-ene-sulfinate (tin sulf).[4] [b] See text for definitions (eqs 1−7).

(**13**)$_2$ (Table 3). Scheme 8 shows the energy profile for the retro-ene reaction of **13** in the presence of BF_3. Interestingly, the S═O bonds of **19** which coordinates BF_3 are not gauche with respect to σ(C(1)−C(2)), as it is the case for complex **17**. The two S−O−H groups are gauche with respects to σ(C(1)−C(2)) and relatively important electrostatic interaction between S−OH and F−B contribute to the high stability of this tetramolecular complex (see Scheme 9). Weak complexes $SO_2\cdots BF_3$,[157] $SO_2\cdots$propene, and $BF_3\cdots$propene, located on the PES, resulted higher in Gibbs free energy than products (BF_3 + SO_2 + propene) and, consequently, they were not included in the ΔG profile shown in Scheme 8.

For the two lowest lying transition states **T8** and **T9** which can be formally viewed as transition structures **T2** and **T3**, respectively, coordinated to BF_3 by interaction of the S═O moiety with the boron center of BF_3, we calculated activation free enthalpies of 8.3 and 12.3 kcal/mol with respect to 0.5·(**13**)$_2$ + BF_3. This would correspond to a substantial catalytic effect of BF_3 on the desulfinylation of both monomeric and dimeric forms of **13** if they would not be highly stabilized through coordination with BF_3. In fact, our calculations give $\Delta G^{\ddagger}$(0.5·**19** → **T8**) = 23.8 kcal/mol, thus suggesting a insignificant catalytic effect of BF_3 in CH_2Cl_2 at −15 °C. These calculations suggest that the ene reaction of propene with sulfur dioxide, which is endergonic at −15 °C in CH_2Cl_2/SO_2 mixtures, might become exergonic in the presence of 1 equiv of BF_3. Indeed, when propene was added to a premixed mixture of SO_2 and BF_3 in CD_2Cl_2, a quick reaction occurred already at −78 °C. The ^{1}H NMR spectrum of the crude reaction mixture showed signals of **13** (minor) and those of polymeric material (major). Thus, it should be possible to realize ene reactions of SO_2 with alkenes if a suitable analogue of BF_3 is willing to catalyze them and to form stable complexes with the sulfinic acids formed, without inducing polymerization.

As we had shown that CF_3COOH is a good catalyst for the hetero-Diels−Alder and cheletropic additions of sulfur dioxide,[155,158] we examined whether this protic acid would also catalyze the retro-ene elimination of SO_2 from prop-2-enesulfinic acid. Our calculations are summarized in Table 3 and Figure 6 for the lowest free energy transition states **T10** and **T11** that can be formally seen as **T2** and **T3**, respectively, interacting with CF_3COOH through hydrogen bonding between S═O moiety and OH of CF_3COOH. Weak electrostatic interaction is probably present between C═O of CF_3COOH and one C−H bond of C(1) in **T10** and C(3) in **T11**. Calculated activation free energies are 23.2 and 24.0 kcal/mol for **T10** and **T11**, respectively, what is somewhat lower than for the monomolecular reaction implying transition structures **T2** (24.3 kcal/mol) and **T3** (25.9 kcal/mol), and the bimolecular mechanism involving transition structure **T4** (25.8 kcal/mol) and **T5** (28.4 kcal/mol).

In the particular cases where the retro-ene reactions occur in the presence either of an activating second molecule of sulfinic acid or a molecule of CF_3CO_2H, an alternative pathway was identified on their respective PESs. According to this second mechanism, the molecule accompanying the initial sulfinic acid reactant is not a mere spectator like in the regular mechanism discussed above (see **T4**, **T5** (Table 2, Figure 4), **T10** and **T11** (Table 3, Figure 6) but it plays an active role forming part directly of the reaction coordinate. Indeed, in the case of the reaction in the presence of a CF_3CO_2H molecule, the SO_2H hydrogen in the sulfinic acid species is transferred to the carboxylic group of CF_3CO_2H at the same time that the hydroxylic hydrogen in this latter species is being transferred to the CH_2 terminal group of the prop-2-enesulfinic acid (see **T10′** and **T11′** structures in the Supporting Information). For the retro-ene reaction in the presence of a second molecule of **13**, this alternative mechanism involves the transfer of the SO_2H hydrogen from the reacting **13** to the accompanying molecule **13** and the simultaneous transfer of the SO_2H hydrogen from the accompanying molecule **13** to the propene-like fragment in the reactant **13** (see **T4′** and **T5′** structures in the Supporting Information). According to our calculations (Tables S2 and S4 in the Supporting Information), the above-described alternative mechanism involve much higher energy barriers [$\Delta G_{solv,SMX}$ = 38.1 (**T4′**), 37.8 (**T5′**), 33.1 (**T10′**) and 33.0 (**T11′**) kcal/mol; to be compared with the corresponding values 25.8 (**T4**), 28.4 (**T5**), 23.2 (**T10**) and 24.0 (**T11**)] and can be safely discarded. Obviously, disfavoring entropy contributions must result much larger than the enthalpic stabilizations associated to the O−H$\cdots$O interactions present in the **T4′**, **T5′**, **T10′**, and **T11′** structures. Consequently, such alternative pathways were not included in Tables 2−3. (Structures **T4′**, **T5′**, **T10′**, and **T11′** were initially located at lower levels of theory by Mr. Ruben Meana during a preliminary search on the PES at a very earlier stage of his research.).

Kinetics Analyses of the Desulfinylation of Prop-2-enesulfinic Acid. 1. Experimental Results. Table 4 collects the experimental results of a series of kinetics measurements of the disulfitative retro-ene reaction of prop-2-ene-1sulfinic acid in the presence of different additives (A = CF_3CO_2H, BF_3OMe_2, TBAF, SO_2, C_6D_{12}, and CD_2Cl_2). Experimental details can be found in the Supporting Information.

In the absence of additive **A** (entries 1, 2; Table 4), the rate of appearance of propene (**P**) fitted the following rate law:

$$d[\mathbf{P}]/dt = k'[(\mathbf{13})_2] \quad (1)$$

where k' is the global rate constant corresponding to the process:

$$(\mathbf{13})_2 \underset{k_{-1}\ (\text{fast})}{\overset{k_1}{\rightleftharpoons}} \mathbf{13} + \mathbf{13} \xrightarrow[(\text{slow})]{k'_2} \mathbf{P} + SO_2 + \mathbf{13}$$

Integration of eq 1 gives

$$[\mathbf{P}] = 2C_o(1 - e^{-k't}) \quad (2)$$

with $k' = k'_2K_1$ ($K_1 = k_1/k_{-1}$), and C_o = initial concentration of dimer (**13**)$_2$.

In the presence of additives A = CF_3CO_2H, TBFA, or SO_2 (entries 3, 4, 5, 8, 9; Table 4), the rate of appearance of **P** fitted the following rate law:

$$d[\mathbf{P}]/dt = k'[(\mathbf{13})_2] + k''[(\mathbf{13})_2]^{1/2} \quad (3)$$

where k' and k'' are global rate constants corresponding to the following processes:

$$(\mathbf{13})_2 \underset{k_{-1}\ (\text{fast})}{\overset{k_1}{\rightleftharpoons}} \mathbf{13} + \mathbf{13} \xrightarrow[(\text{slow})]{k'_2} \mathbf{P} + SO_2 + \mathbf{13}$$

with $k' = K_1 k'_2$, and

$$(\mathbf{13})_2 + \mathbf{A} \underset{k_{-1}\ (\text{fast})}{\overset{k_1}{\rightleftharpoons}} \mathbf{13} + \mathbf{13} + \mathbf{A} \xrightarrow[(\text{slow})]{k''_2} \mathbf{P} + SO_2 + \mathbf{13} + \mathbf{A}$$

with $k'' = K_1^{1/2} k''_2[\mathbf{A}]$

Integration of eq 3 gives

$$[P] = 2\left\{C_0 - \left[\frac{(k'' + k'\sqrt{C_0})\exp(-k't/2) - k''}{k'}\right]^2\right\} \quad (4)$$

Experimental [**P**] vs t curves can be found in the Supporting Information. Fittings to eqs 2 and 4 provide the values for k' and k'' rate constants collected in Table 4.

In Figure 7 are presented four kinetics for the decay of prop-2-enesulfinic acid in the retroene reaction. In absence of any

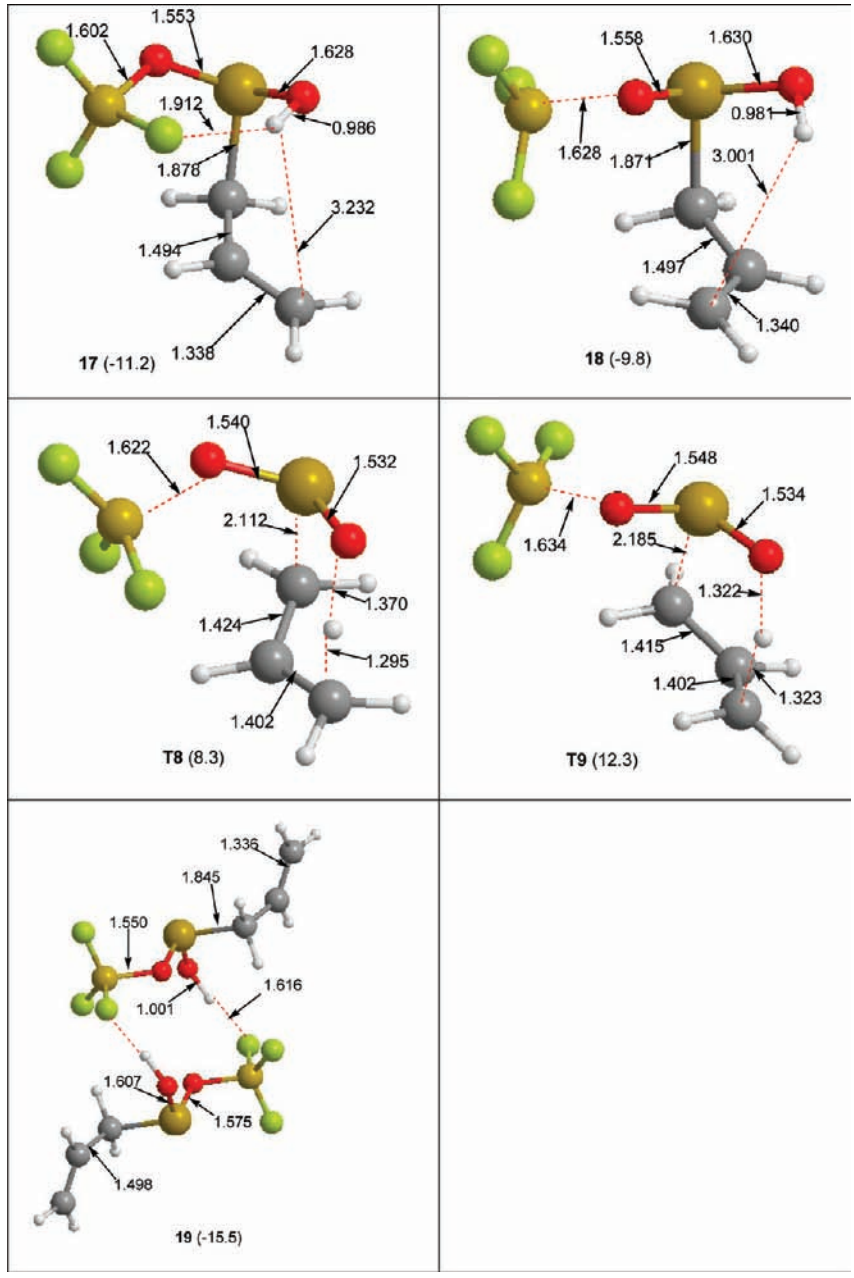

Figure 5. B3LYP/6-31+G(d,p) structures of the species located on the PES of the retro-ene reaction of **13** in the presence of BF_3. Some selected bond distances are given in Å. CCSD(T)/6-311+G(d,p)//B3LYP//6-31+G(d,p) Gibbs free energy differences, including solvent effects, with respect to 0.5·$(\mathbf{13})_2$ (Table 3).

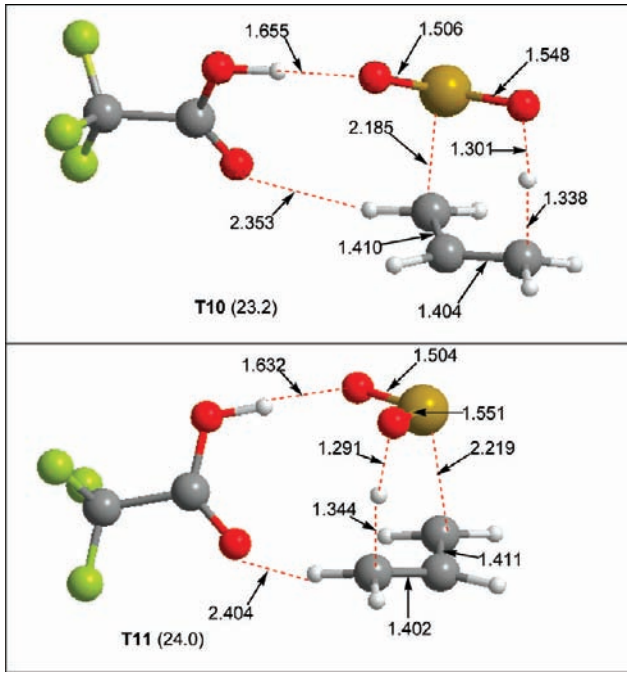

Figure 6. B3LYP/6-31+G(d,p) transition structures located on the PES of the retro-ene reaction of **13** in the presence of one molecule of CF_3COOH. Some selected bond distances are given in Å. CCSD(T)/6-311+G(d,p)//B3LYP//6-31+G(d,p) Gibbs free energy differences, including solvent effects, with respect to 0.5·(**13**)$_2$ (Table 3).

additive, Figure 7a and b, the kinetics follows first order decay with rate law values fitted as $k'_a = 0.00575\ min^{-1}$ ($R^2_a = 0.98313$) and $k'_b = 0.00565\ min^{-1}$ ($R^2_b = 0.99482$). Figure 7c and d represents decay of prop-2-enesulfinic acid with 0.19 or 0.88 equiv of TFA as additive. If these kinetics are fitted with equations combining mixed half and first order rate laws the R^2 value are $R^2_c = 0.99904$ and $R^2_d = 0.9984$, respectively, and the rate constant values are $k'_c = 0.00578\ min^{-1}$ and $k''_c = 0.00055\ mol^{1/2}/kg^{1/2}\cdot min$ and $k'_d = 0.00564\ min^{-1}$ and $k''_d = 0.00335\ mol^{1/2}/kg^{1/2}\cdot min$, respectively. When the decay is fitted as first rate law the R^2 value are smaller and found to amount to $R^2_c = 0.99791$ and $R^2_d = 0.99659$, respectively.

Theoretical Analysis. A. Half-order mechanism for the desulfinylation of the dimer (1st-order mechanism in the monomer). Our calculations suggest that a pre-equilibrium between **13** and its dimer (**13**)$_2$ is established very fast. Indeed, no energy barrier for the dimer formation was detected on the PES. A double hydrogen-bonding-like interaction (Figure 2) with S−OH···H bond distances of 1.631 Å is responsible for the dimer stabilization. The energy profile arising from our calculations (see Scheme 6) suggests a half-order in the sulfinic acid dimer (first-order rate law in the sulfinic acid monomer) defined by Scheme 10.

According to our calculations (see Table 2), (**13**)$_2$ is about 3−5 kcal/mol more stable than the corresponding monomer **13** in any of the two conformations **13a** or **13b** at −15° in CH_2Cl_2. Conformers **13a** and **13b** interconvert in each other through a transition structure (see **T1** in Figure 1 and Scheme 3) involving a small barrier of less than 5 kcal/mol (Table 2).

B. First-Order Mechanism for the Desulfinylation of the Dimer (Second-Order Mechanism in the Monomer). Let us now consider the possibility that two molecules of **13** take part in the process according to a first-order mechanism in the sulfinic acid dimer (second-order mechanism in the monomer) defined by Scheme 11.

Two molecules of **13** as conformers **13a** or **13b** interact with each other giving rise to the products of the retro-ene process (SO_2 + propene + 1/2 dimer) through transition structures **T4** and **T5** (Table 2, Figure 4), respectively. One of the molecules plays the role of activator and the second molecule undergoes itself the rearrangements required to render the retro-ene products in a concerted way as described above.

As pointed out in a previous section, the activation free energy for the bimolecular mechanism, $\Delta G_{solv,SMX}^{\ddagger}$(**T4**) = 25.8 kcal/mol, is slightly larger than the corresponding value for the monomolecular mechanism, $\Delta G_{solv,SMX}^{\ddagger}$(**T2**) = 24.3 kcal/mol. This theoretical prediction apparently contradicts the experimental evidence (see Table 4) which shows that the retro-ene reaction of **13** is a first-order reaction in the dimer with a reaction rate constant of $k_{global} = 5.7 \times 10^{-3}\ min^{-1}$. However, one must take into consideration the fact that the structure of the transition structures defining the first-order mechanism, **T4** and **T5**, are conformationally very complex. In fact, Figure 8 collects the 24 different conformations **a**···**x**, all of them energetically close to each other (25.3−26.3 kcal/mol), adopted by **T4**. There are another 24 equivalent structures for **T5** (Table 5) (see Figures

Scheme 8. CCSD(T)/6-31+G(d,p)//B3LYP/6-31+G(d,p) + SM5.43R ΔG Profile

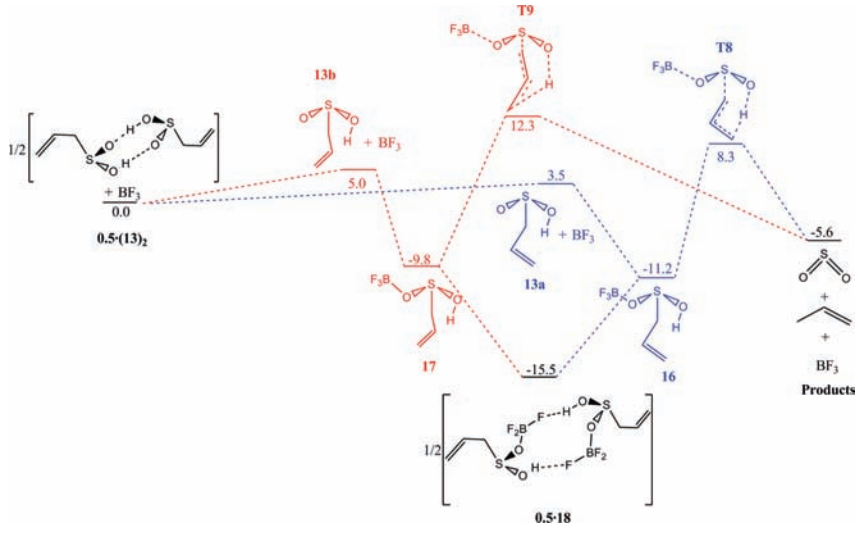

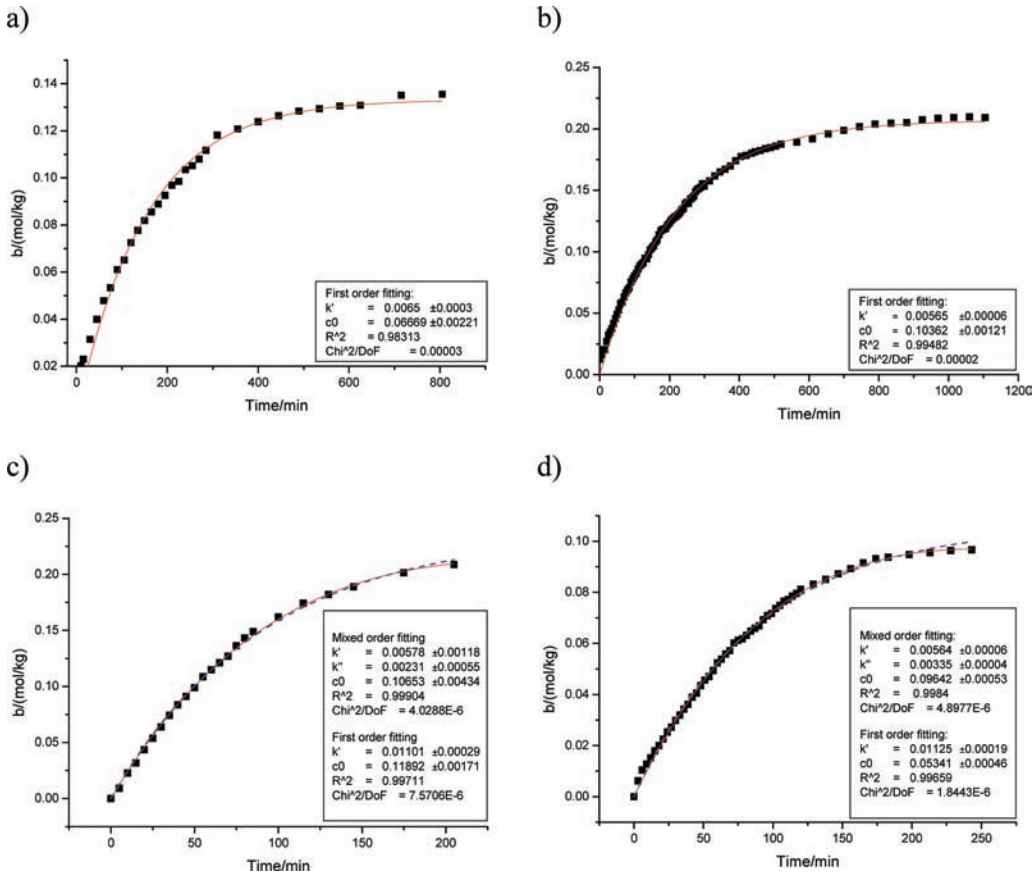

Figure 7. Appearance of prop-1-ene at −15 °C arising from a mixtures made of 0.47 equiv of TFA to allyl tributyltin sulfinate (**S1**). (a) *n*(TFA)/*n*(prop-2-enesulfinic acid) = 0.47 red line represent first order fitting. (b) *n*(TFA)/*n*(prop-2-enesulfinic acid) = 0.86 red line represents first-order fitting. (c) *n*(TFA)/*n*(prop-2-enesulfinic acid) = 1.19 red line represent mixed order fitting (dotted line first-order fitting). (d) *n*(TFA)/*n*(prop-2-enesulfinic acid) = 1.88 red line represent mixed order fitting (dotted line first-order fitting).

Scheme 9

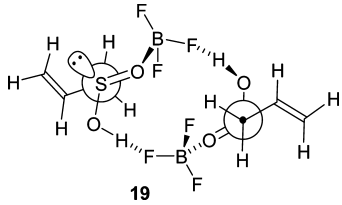

19

Scheme 10. Monomolecular Mechanism

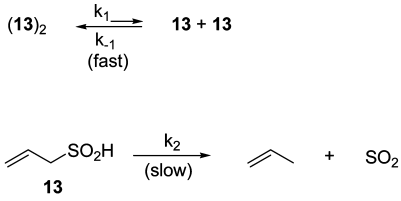

$$K_1 = \frac{k_1}{k_{-1}} = \frac{[13]^2}{[(13)_2]}$$

$$-\frac{d[(13)_2]}{dt} = \frac{d[propene]}{dt} = K_1^{1/2} \cdot k_2 \cdot [(13)_2]^{1/2} = k \cdot [(13)_2]^{1/2} \quad (5)$$

S1−S2 of the Supporting Information) on the PES, all of them contributing to the rate constant. We have employed the CTST theory[127] to get a rough estimate of the theoretically predicted reaction rate constants both in the gas phase and in solution. As can be seen in Table 5, the global rate constant for the first-order rate law in the dimer becomes 1.65×10^{-5} min^{-1} (transmission coefficient, $\kappa = 11.065$, was computed using the SCT approximation).[128] This value should be compared with

Scheme 11. Bimolecular Mechanism

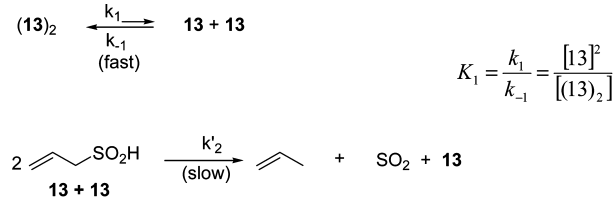

$$K_1 = \frac{k_1}{k_{-1}} = \frac{[13]^2}{[(13)_2]}$$

$$-\frac{d[(13)_2]}{dt} = \frac{d[propene]}{dt} = K_1 \cdot k'_2 \cdot [(13)_2] = k' \cdot [(13)_2] \quad (6)$$

the CTST estimate of the rate constant for a half-order mechanism in the dimer which, after tunnelling corrections ($\kappa = 18.611$), becomes 1.45×10^{-5} $mol^{1/2}/kg^{1/2} \cdot min$. Thus, while our calculations suggest a mixed half-order + first-order kinetics in the dimer, experimental fittings (see Table 4) shows that desulfinylation of **13** proceeds through a first-order mechanism in the dimer $(\mathbf{13})_2$. It is clear that our theoretical predictions cannot reach the very high level of accuracy required to discern the subtle factors controlling the change from a mixed half-order + first-order mechanism to a full first-order mechanism. In this context, let us just mention a few well-known drawbacks associated with the theoretical treatments: (a) for quite different reasons,[159,160] theoretical kinetics predictions are far from being a trivial task, even for relatively simple small-sized gas phase

(156) Suarez, D.; Sordo, T. L.; Sordo, J. A. *J. Am. Chem. Soc.* **1994**, *116*, 763–764.

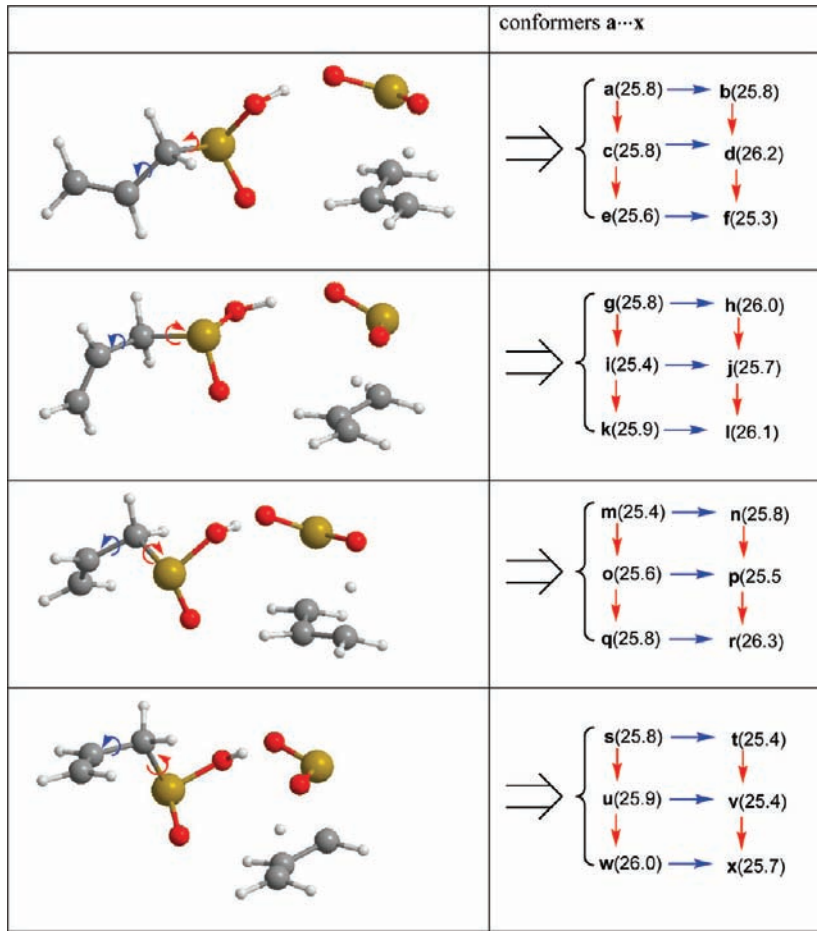

Figure 8. Twenty-four possible conformers (**a···x**) of similar relative free energies generated by rotation about the C(1)−S bond (red arrows) and about the C(1)−C(2) bond (blue arrows) for transition structure **T4** ("autocatalysis"). In parentheses, CCSD(T)/6-311+G(d,p)//B3LYP//6-31+G(d,p) Gibbs free energy differences.

systems. One of the most critical factors is that kinetics predictions do involve the calculation of the $\exp(-\Delta G^{\ddagger}/RT)$ factor in the CTST mathematical expression for the rate constant.[127] Thus, relatively small errors in the theoretical estimate of $\Delta G^{\ddagger}$ do produce considerable deviations in the predicted rate constants. A trivial calculation tells us that an error in 1 kcal/mol in $\Delta G^{\ddagger}$ (the goal, not always achieved at all, in today's theoretical thermodynamic predictions for small-sized systems)[161−165] gives rise to a discrepancy in 1 order of magnitude in the rate constant. Thus, the discrepancies between theoretically predicted (Table 5) and experimentally determined (Table 4) rate constants, represent about 2 kcal/mol error in the calculation of $\Delta G^{\ddagger}$ which, according to our own experience,[161−163] is the best level of accuracy attainable with today's software and hardware utilities affordable for the kind of systems (number of electrons) dealt with in the present study. These unavoidable discrepancies between experimentally measured and theoretically predicted rate constants, that have been emphasized in recent works (see, for example, refs 166−168), should be kept in mind when assessing and judging the appropriateness of a given theoretical treatment. (b) As can be inferred from inspection of Table 5, solvent effects exert a remarkable influence on the $\Delta G^{\ddagger}$ and k values. Despite the fact we employed a theoretical model recently developed to properly account for solvent effects,[124,125] limitations inherent to the solvent theoretical models are still considerable,[122] and (c) although impressive advances in the accuracy of DFT methodologies have been accomplished during the past few years,[169] it is clear that the simultaneous accurate representation of kinetics and thermodynamics for a given process like the one studied here, is not a trivial task.[170] We decided to carry out the geometry optimizations by using the most popular and widely employed DFT functional:

(157) Peebles, S. A.; Sun, L.; Kuczkowski, R. L.; Nxumalo, L. M.; Ford, T. A. *J. Mol. Struct.* **1998**, *471*, 235–242.
(158) Roversi, E.; Scopelliti, R.; Solari, E.; Estoppey, R.; Vogel, P.; Braña, P.; Menendez, B.; Sordo, J. A. *Chem.—Eur. J.* **2002**, *8*, 1336–1355.
(159) Cimas, A.; Rayon, V. M.; Aschi, M.; Barrientos, C.; Sordo, J. A.; Largo, A. *J. Chem. Phys.* **2005**, *123*, 114312−1–114312/11.
(160) Gonzalez-Lafont, A.; Lluch, J. M.; Varela-Alvarez, A.; Sordo, J. A. *J. Phys. Chem. B* **2008**, *112*, 328–335.
(161) Feller, D.; Sordo, J. A. *J. Chem. Phys.* **2000**, *112*, 5604–5610.
(162) Feller, D.; Sordo, J. A. *J. Chem. Phys.* **2000**, *113*, 485–493.
(163) Sordo, J. A. *J. Chem. Phys.* **2001**, *114*, 1974–1980.
(164) Feller, D.; Peterson, K. A.; de Jong, W. A.; Dixon, D. A. *J. Chem. Phys.* **2003**, *118*, 3510–3522.
(165) Feller, D.; Peterson, K. A.; Crawford, T. D. *J. Chem. Phys.* **2006**, *124*, 054107−1–054107/17.
(166) Golden, D. M.; Barker, J. R.; Lohr, L. L. *J. Phys. Chem. A* **2003**, *107*, 11057–11071.
(167) Maranzana, A.; Barker, J. R.; Tonachini, G. *Phys. Chem. Chem. Phys.* **2007**, *9*, 4129–4141.
(168) Maranzana, A.; Barker, J. R.; Tonachini, G. *J. Phys. Chem. A* **2008**, *112*, 3666–3675.
(169) Sousa, S. F.; Fernandes, P. A.; Ramos, M. J. *J. Phys. Chem. A* **2007**, *111*, 10439–10452.
(170) Zhao, Y.; Schultz, N. E.; Truhlar, D. G. *J. Chem. Theory Comput.* **2006**, *2*, 364–382.

Table 5. Gas-Phase and Solution Gibbs Free Energies (kcal/mol) for the 48 Transition Structures Located on the PES for the First-Order Mechanism in the Sulfinic Acid Dimer As Computed at the CCSD(T)/6-311+G(d,p)//B3LYP/6-31+G(d,p) Level, Using the Standard State 1 M at 258.15 K[a]

structure	ΔG(gas)	k(gas)	$\Delta G_{solv,SMX}$	k(solv)
T4-a	28.4	3.24×10^{-09}	25.8	5.14×10^{-07}
T4-b	28.7	1.80×10^{-09}	25.8	5.14×10^{-07}
T4-c	29.0	1.00×10^{-09}	26.2	2.36×10^{-07}
T4-d	28.2	4.78×10^{-09}	25.6	7.59×10^{-07}
T4-e	28.4	3.24×10^{-09}	25.3	1.36×10^{-06}
T4-f	29.0	1.00×10^{-09}	25.8	5.14×10^{-07}
T4-g	28.8	1.48×10^{-09}	26.0	3.48×10^{-07}
T4-h	28.0	7.06×10^{-09}	25.4	1.12×10^{-06}
T4-i	28.1	5.81×10^{-09}	25.7	6.25×10^{-07}
T4-j	28.6	2.19×10^{-09}	25.9	4.23×10^{-07}
T4-k	29.0	1.00×10^{-09}	26.1	2.87×10^{-07}
T4-l	28.2	4.78×10^{-09}	25.4	1.12×10^{-06}
T4-m	28.5	2.66×10^{-09}	25.8	5.14×10^{-07}
T4-n	27.9	8.58×10^{-09}	25.6	7.59×10^{-07}
T4-o	27.9	8.58×10^{-09}	25.5	9.23×10^{-07}
T4-p	28.3	3.93×10^{-09}	25.8	5.14×10^{-07}
T4-q	29.3	5.60×10^{-10}	26.3	1.94×10^{-07}
T4-r	28.6	2.19×10^{-09}	25.8	5.14×10^{-07}
T4-s	27.9	8.58×10^{-09}	25.4	1.12×10^{-06}
T4-t	28.1	5.81×10^{-09}	25.9	4.23×10^{-07}
T4-u	27.6	1.54×10^{-08}	25.4	1.12×10^{-06}
T4-v	28.1	5.81×10^{-09}	25.9	4.23×10^{-07}
T4-w	28.7	1.80×10^{-09}	26.0	3.48×10^{-07}
T4-x	28.2	4.78×10^{-09}	25.7	6.25×10^{-07}
T5-a	30.4	6.56×10^{-11}	28.4	3.24×10^{-09}
T5-b	29.8	2.11×10^{-10}	28.1	5.81×10^{-09}
T5-c	29.7	2.57×10^{-10}	27.9	8.58×10^{-09}
T5-d	30.6	4.44×10^{-11}	28.6	2.19×10^{-09}
T5-e	30.5	5.40×10^{-11}	28.2	4.78×10^{-09}
T5-f	29.8	2.11×10^{-10}	27.7	1.27×10^{-08}
T5-g	29.0	1.00×10^{-09}	27.6	1.54×10^{-08}
T5-h	29.6	3.12×10^{-10}	27.8	1.04×10^{-08}
T5-i	29.6	3.12×10^{-10}	27.9	8.58×10^{-09}
T5-j	29.3	5.60×10^{-10}	27.8	1.04×10^{-08}
T5-k	29.9	1.74×10^{-10}	27.9	8.58×10^{-09}
T5-l	30.1	1.18×10^{-10}	28.0	7.06×10^{-09}
T5-m	29.3	5.60×10^{-10}	27.7	1.27×10^{-08}
T5-n	29.1	8.27×10^{-10}	27.5	1.87×10^{-08}
T5-o	29.1	8.27×10^{-10}	27.5	1.87×10^{-08}
T5-p	29.4	4.61×10^{-10}	27.7	1.27×10^{-08}
T5-q	29.7	2.57×10^{-10}	27.8	1.04×10^{-08}
T5-r	30.0	1.43×10^{-10}	28.1	5.81×10^{-09}
T5-s	29.9	1.74×10^{-10}	27.8	1.04×10^{-08}
T5-t	30.6	4.44×10^{-11}	28.2	4.78×10^{-09}
T5-u	30.6	4.44×10^{-11}	28.1	5.81×10^{-09}
T5-v	30.0	1.43×10^{-10}	27.8	1.04×10^{-08}
T5-w	28.7	2.80×10^{-09}	26.3	1.94×10^{-07}
T5-x	28.0	7.06×10^{-09}	25.6	7.59×10^{-07}
total		1.22×10^{-07}		1.65×10^{-05}

[a] The corresponding CTST rate constants (min^{-1}) are also included (tunnel contributions were estimated with the SCT approximation).

B3LYP.[118−120] Although some of its shortcomings in predicting stabilities or kinetic barriers[170] are expected to be overcome through the CCSD(T)//DFT(B3LYP) single-point calculations we carried out, unavoidable inaccuracies in the geometrical parameters must necessarily accompany the energy predictions. Bearing in mind the above limitations, we consider that the degree of agreement between theoretical and experimental rate constants reached in the present work is rather acceptable.

C. Desulfinylation in the Presence of SO_2 or CF_3CO_2H. The possibility of catalysis for the retro-ene reaction of **13** acid was explored by analyzing the effect of the presence of additive **A** such as SO_2 or CF_3CO_2H. The structures located on the PES (Table 3) suggest the mechanism in Scheme 12.

Scheme 12. Mechanism of the Desulfinylation in the Presence of Additive SO_2 or CF_3COOH

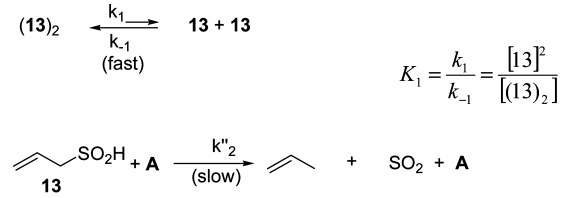

$$K_1 = \frac{k_1}{k_{-1}} = \frac{[13]^2}{[(13)_2]}$$

$$-\frac{d[(13)_2]}{dt} = \frac{d[propene]}{dt} = K_1^{1/2} \cdot k''_2 \cdot [(13)_2]^{1/2} = k'' \cdot [(13)_2]^{1/2} \quad (7)$$

Transition structures **T6** (25.2 kcal/mol) and **T7** (25.4 kcal/mol) for the retro-ene reaction in the presence of SO_2 (see Table 3, Figure 4) are slightly higher than the energy barriers of the desulfinylation reaction in the absence of SO_2 (Table 2). Therefore, calculations suggest that SO_2 does not catalyze the reaction **13** → propene + SO_2, in agreement with experimental data (Table 4).

In the presence of CF_3CO_2H, the free energy of activation (see Table 3) becomes slightly lower: 23.2 (**T10**) and 24.0 (**T11**) kcal/mol, thus suggesting a moderate catalytic effect which is also consistent with experimental data collected in Table 4. The estimated global rate constant for the kinetic law equation in eq 3 becomes 8.85×10^{-5} $mol^{1/2}/kg^{1/2} \cdot min$, which, bearing in mind the theoretical limitations to make quantitative kinetics predictions mentioned in the preceding section, agrees reasonably well with the experimentally estimated rate constant of 9.38×10^{-3} $mol^{1/2}/kg^{1/2} \cdot min$.

D. Desulfinylation in the Presence of $BF_3 \cdot Me_2O$. The free energy diagram for the desulfinylation of **13** in the presence of BF_3 is somewhat more complicated (see Scheme 8) than those for the other reactions presented above. This is due to the fact that BF_3 generates with **13** two relatively stable complexes **17** and **18** and, more importantly, the tetramolecular complex **19** (Table 3, Figure 5). No data have been reported yet for the enthalpies of complex formation of BF_3 with sulfinic acids. The enthalpy change for the reaction of gaseous BF_3 and Et_2O in CH_2Cl_2 has been measured to amount to −18.8 kcal/mol. With MeSOMe in CH_2Cl_2, the reaction is more exothermic and gives a heat of complex formation of −25.7 kcal/mol.[171] Thus, if sulfoxides can be considered to mimick sulfinic acids for their Lewis basicity, it is expected that $BF_3 \cdot Me_2O$, the additive employed in our experiments instead of BF_3, will form stable complex with dimeric $(\mathbf{13})_2$, producing **19**. By manometric measurements, McLaughlin and Tamres,[172] determined for liquid $BF_3 \cdot Me_2O$ a heat of complex formation of −13.65 ± 0.2 kcal/mol (25 °C) and an entropy of complex formation of −33.1 ± 0.6 e.u. (25 °C). −15 °C (our reaction conditions) $\Delta G = -13650 - 258.15(-33.1) \cong -5.1$ kcal/mol.

Then,

$$BF_3 + Me_2O \rightleftarrows BF_3 \cdot Me_2O \quad \Delta G = -5.1 \text{kcal/mol}$$

On the other hand, according to our calculations (see Table 2 and Scheme 5),

$$BF_3 + 0.5(\mathbf{13})_2 \rightleftarrows 0.5(\mathbf{19}) \quad \Delta G = -15.5 \text{kcal/mol}$$

and consequently,

$$0.5(\mathbf{13})_2 + BF_3 \cdot Me_2O \rightleftarrows 0.5(\mathbf{19}) + Me_2O \quad \Delta G = -10.4 \text{kcal/mol}$$

Therefore, the real stability of **19**, with respect to products, when employing $BF_3 \cdot Me_2O$ instead of BF_3, will be about 5 kcal/mol. This result is a very relevant theoretical prediction which allows us to interpret the experimental observation (see Table 4) that the retro-ene reaction in the presence of $BF_3 \cdot Me_2O$ is inhibited as the amount of the latter increases. Indeed, the formation of **19** is a competitive process with respect to the retro-ene reaction (see Scheme 8). The greater exergonicity for the formation of **19** will inhibit the formation of the retro-ene products (SO_2 + propene), in agreement with the experimental observation.

Conclusion

13 in CH_2Cl_2 solution at −15 °C equilibrates with a dimeric form $(\mathbf{13})_2$ which undergoes the retro-ene elimination of SO_2 with production of propene and 1 equiv of **13**. In the transition state of this one-step, concerted reaction, one molecule of sulfinic acid makes a hydrogen bond with the S═O moiety of the molecule undergoing the pericyclic reaction. Although protic acids such as CF_3COOH, or Lewis acids such as SO_2 are known to catalyze other pericyclic reactions of SO_2 such as the hetero-Diels−Alder and cheletropic additions to 1,3-dienes, these acids are not efficient catalysts of the retro-ene elimination of SO_2. In the presence of catalytic amount of $BF_3 \cdot Me_2O$ the reaction is almost not affected. When using a large amount of $BF_3 \cdot Me_2O$, the reaction is completely inhibited because of the formation of a stable tetramolecular complex of type (prop-2-enesulfinic acid)$_2$, $(BF_3)_2$ (**19**). Quantum calculations suggest concerted retro-ene elimination of SO_2 from prop-2-enesulfinic acid with transition states in which the C(1)···S bond elongation and the S−O···H···C(3) transfer occurs in concert, and this independently of the nature of the additive that interacts with the S═O moiety. The favored transition states adopt six-membered, chairlike structures in which the S═O moieties is gauche with σ(C(1)−C(2)) bond of the propenyl unit (S═O occupies an pseudoaxial position). This stabilizing gauche effect involving a polar S═O and less polar C−C bond is also found in **13** in CH_2Cl_2 solution, in its dimeric form $(\mathbf{13})_2$. This is not the case anymore in complex **19** in which the SOH/σ(C(1)−C(2)) are gauche. Contrary to the reaction of S═O with alkenes that generate thiirane oxides, and that of SO_3 which give products of ene-reaction via β-sultone intermediates, the ene-reaction of SO_2 with alkene does not follow mechanisms in which either thiirane 1,1-dioxide of β-sultane would be intermediates. In fact the retro-ene elimination of SO_2 from prop-2-enesulfinic acid follows a converted mechanisms in which the hydrogen atom transfer is rate-determining as for the thermal decarboxylation of but-3-enoic acid into propene + CO_2, and the thermal fragmentations of β,γ-unsaturated carbonyl imine and diazene compounds into alkenes- + RR′C═O, RR′C═NH, and N_2, respectively. The exergonic ene-reaction of SO_2 with alkenes follows the same mechanism as the ene-reaction of SeO_2 with alkenes.

Acknowledgment. We thank the Swiss National Science Foundation, the Roche Research Foundation, the "Secrétariat d'Etat à l'Education et à la Recherche (SER), the CSCS (Manno, Switzerland), MEC (Madrid, Spain, Project No. CTQ 2007-67234-C02-01/BQU), and FICYT (Gobierno del Principado de Asturias, Project No. IB08-023) for financial support. A long time ago, Mr. Florentino Fernandez performed a preliminary exploration of the PESs corresponding to the retro-ene reaction of prop-2-enesulfinic acid in the presence of SO_2, BF_3, HF, and H_3O^+ by employing lower levels of theory. Mr Ruben Meana located some structures, included in the Supporting Information section, corresponding to an alternative mechanism for the case of the presence of TFA or a second molecule of sulfinic acid. We thank all such contributions at the very early stages of this research.

Supporting Information Available: Calculated CCSD(T)/6-311 + G(d,p)//B3LYP/6-31 + G(d,g) absolute energy values for prop-2-enesulfinic acid and its dimer, intermediates pre- and post-transition state complexes and transition structures, in the absence or presence of additives (SO_2, BF_3, CF_3COOH) (Tables S1−S5). Representations of all possible conformers of bimolecular transition structures **T4a-x**, **T5a-x** (Figures S1−S2). ^{1}H NMR spectra of **13** + $BF_3 \cdot Me_2O$ in CD_2Cl_2/toluene internal reference. Experimental details on the preparation of **13** and on the kinetic measurements and sample preparations (Figures S3−S11). Complete ref 129. This material is available free of charge via the Internet at http://pubs.acs.org.

JA901565S

(171) Maria, P. C.; Gal, J. F. *J. Phys. Chem.* **1985**, *89*, 1296–1304.
(172) McLaughlin, D. E.; Tamres, M. *J. Am. Chem. Soc.* **1960**, *82*, 5618–5621.